

University of Montana

## ScholarWorks at University of Montana

---

Graduate Student Theses, Dissertations, &  
Professional Papers

Graduate School

---

2005

### Synthesis of novel N-aryl asparagine analogues as inhibitors of glutamine transport by the neutral amino acid transporter SN1

Christopher Andrew Timko  
*The University of Montana*

Follow this and additional works at: <https://scholarworks.umt.edu/etd>

**Let us know how access to this document benefits you.**

---

#### Recommended Citation

Timko, Christopher Andrew, "Synthesis of novel N-aryl asparagine analogues as inhibitors of glutamine transport by the neutral amino acid transporter SN1" (2005). *Graduate Student Theses, Dissertations, & Professional Papers*. 6643.

<https://scholarworks.umt.edu/etd/6643>

This Thesis is brought to you for free and open access by the Graduate School at ScholarWorks at University of Montana. It has been accepted for inclusion in Graduate Student Theses, Dissertations, & Professional Papers by an authorized administrator of ScholarWorks at University of Montana. For more information, please contact [scholarworks@mso.umt.edu](mailto:scholarworks@mso.umt.edu).



**Maureen and Mike  
MANSFIELD LIBRARY**

The University of  
**Montana**

---

Permission is granted by the author to reproduce this material in its entirety, provided that this material is used for scholarly purposes and is properly cited in published works and reports.

**\*\*Please check "Yes" or "No" and provide signature\*\***

Yes, I grant permission

No, I do not grant permission

Author's Signature: \_\_\_\_\_

*Christopher J. Lingo*

Date: \_\_\_\_\_

*Dec 9, 2005*

Any copying for commercial purposes or financial gain may be undertaken only with the author's explicit consent.

---



**SYNTHESIS OF NOVEL N-ARYL ASPARAGINE ANALOGUES AS INHIBITORS OF GLUTAMINE  
TRANSPORT BY THE NEUTRAL AMINO ACID TRANSPORTER SN1**

by

**Christopher Andrew Timko**

**B.S. The University of the South, Sewanee, Tennessee 2002**

**presented in partial fulfillment of the requirements**

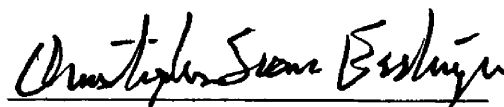
**for the degree of**

**Master of Science**

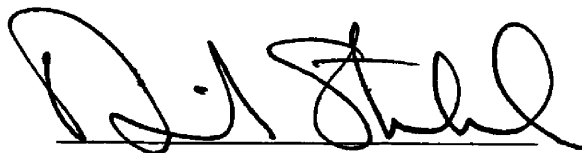
**The University of Montana**

**December 2005**

Approved by:



Chairperson



Dean, Graduate School

12-23-05

Date

UMI Number: EP37444

All rights reserved

**INFORMATION TO ALL USERS**

The quality of this reproduction is dependent upon the quality of the copy submitted.

In the unlikely event that the author did not send a complete manuscript and there are missing pages, these will be noted. Also, if material had to be removed, a note will indicate the deletion.



UMI EP37444

Published by ProQuest LLC (2013). Copyright in the Dissertation held by the Author.

Microform Edition © ProQuest LLC.

All rights reserved. This work is protected against unauthorized copying under Title 17, United States Code



ProQuest LLC.  
789 East Eisenhower Parkway  
P.O. Box 1346  
Ann Arbor, MI 48106 - 1346

Timko, Christopher A., M.S., December 2005

Chemistry

**Synthesis of Novel N-Aryl Asparagine Analogues as Inhibitors of Glutamine Transport by the Neutral Amino Acid Transporter SN1**

Committee Chair: Dr. C. Sean Esslinger CSE

Recent studies have shown that glutamine transport in adult brain is mediated predominantly by system N transporter (SN1, NAT, g17, SNAT3, SLC38A3) in astrocytes and system A transporter (SA2, ATA1, SAT1, GlnT, NAT2, SNAT1, SLC38A1) in neurons. These glutamine transporters are in the same family and thus fairly similar in function. Although N-methyl amino isobutyric acid (MeAIB) inhibits the transport of glutamine through system A, there are no selective inhibitors for system N (specifically SN1). A potent small molecule inhibitor would greatly help elucidate the role of this protein with respect to glutamate neurotransmission. Based on previous structure activity relationships and computer modeling of natural substrates for SN1, a family of N-aryl asparagine analogues have been designed and synthesized to fill this gap in the current research. These asparagine compounds will help create a more detailed binding site map for the SN1 transporter and open the door for even more potent inhibitors.

Timko, Christopher A., M.S., December 2005

Chemistry

**Synthesis of Novel N-Aryl Asparagine Analogues as Inhibitors of Glutamine Transport by the Neutral Amino Acid Transporter SN1**

Committee Chair: Dr. C. Sean Esslinger CSE

Recent studies have shown that glutamine transport in adult brain is mediated predominantly by system N transporter (SN1, NAT, g17, SNAT3, SLC38A3) in astrocytes and system A transporter (SA2, ATA1, SAT1, GlnT, NAT2, SNAT1, SLC38A1) in neurons. These glutamine transporters are in the same family and thus fairly similar in function. Although N-methyl amino isobutyric acid (MeAIB) inhibits the transport of glutamine through system A, there are no selective inhibitors for system N (specifically SN1). A potent small molecule inhibitor would greatly help elucidate the role of this protein with respect to glutamate neurotransmission. Based on previous structure activity relationships and computer modeling of natural substrates for SN1, a family of N-aryl asparagine analogues have been designed and synthesized to fill this gap in the current research. These asparagine compounds will help create a more detailed binding site map for the SN1 transporter and open the door for even more potent inhibitors.

## Table of Contents:

<b>Abstract</b>	<b>ii</b>
<b>Introduction</b>	<b>1</b>
<b>Discussion</b>	<b>12</b>
<b>Conclusion</b>	<b>27</b>
<b>Experimental</b>	<b>29</b>
<b>References</b>	<b>53</b>
<b>Appendices</b>	<b>56</b>



**List of Tables:**

**Table 1: Comparison of observational TLC data for beta/alpha**

**ratio of amide formation using six different solvent systems.**

**17**

## List of Figures:

<b>Figure 1: Glutamine/glutamate cycle</b>	<b>2</b>
<b>Figure 2: Uncoupled proton channel</b>	<b>5</b>
<b>Figure 3: Different flux situations for SN1 transport of glutamine</b>	<b>7</b>
<b>Figure 4: The three natural substrates transported by SN1</b>	<b>8</b>
<b>Figure 5: The initial SN1 transporter binding site map</b>	<b>9</b>
<b>Figure 6: N-aryl glutamine analogues</b>	<b>9</b>
<b>Figure 7: The family of asparagine analogues to be synthesized</b>	<b>10</b>
<b>Figure 8: Future directions for synthetic analogues</b>	<b>11</b>
<b>Figure 9: Rational for the preference of alpha addition in certain solvents</b>	<b>15</b>
<b>Figure 10: The alpha-O-benzyl mono protected Boc-L-aspartamide</b>	<b>24</b>
<b>Figure 11: Synthetic modification to improve to improve yields for beta amides</b>	<b>28</b>

## List of Schemes:

<b>Scheme 1: Original synthetic route through aspartic anhydride</b>	<b>12</b>
<b>Scheme 2: Anhydride reaction produces alpha and beta addition</b>	<b>13</b>
<b>Scheme 3: Reaction scheme that uses the trityl protecting group to specifically form beta amides</b>	<b>19</b>
<b>Scheme 4: DCC adduct can rearrange to inactive adduct</b>	<b>20</b>
<b>Scheme 5: Changing protection groups to allow for acid chloride synthetic step</b>	<b>22</b>
<b>Scheme 6: Hydrolysis of methyl ester causes ring closing that opens to create a mixture of alpha and beta amides</b>	<b>23</b>
<b>Scheme 7: Aspartic anhydride reaction with naphthylamine using ethanol as the solvent</b>	<b>25</b>
<b>Scheme 8: Deprotection steps to produce target asparagine analogues</b>	<b>26</b>
<b>Scheme 9: The synthetic route developed for aromatic asparagine analogues</b>	<b>28</b>

## **Introduction:**

L-glutamine composes one-fifth of all the free amino acids present in blood plasma and two thirds of the amino acids in cerebrospinal fluid (CSF) [McGale et al. 1977]. Glutamine itself does not directly cause signaling in the brain but experiments support that glutamine is a major precursor to the neurotransmitter glutamate through the enzyme glutaminase and the glutamine/glutamate cycle. Glutamate is then a precursor for gamma-aminobutyric acid (GABA), through the tricarboxylic acid cycle [Bröer et al. 2004]. Glutamate and gamma-aminobutyric acid are, respectively, the main excitatory and inhibitory neurotransmitters in the brain [Deitmer et al. 2003].

The process by which glutamine regenerates the glutamate supply is called the glutamine/glutamate cycle. The glutamine/glutamate cycle involves the vesicular release of glutamate from the presynaptic neuron into the synaptic cleft. Glutamate is then taken up into astrocytes by the glutamate transporter EAAT2 where glutamate is converted into glutamine by the enzyme glutamine synthetase. Glutamine is then released into the CSF by the SN1 transporter and then taken up into the neuron by the system A transporter or ATA1. In the neuron the glutamine is converted into glutamate by the enzyme glutaminase and then packaged into vesicles by VGLUT, a vesicular glutamate transporter, and the cycle begins again [Bröer et al. 2001]. The glutamine/glutamate cycle allows for glutamate, which is potentially excitotoxic in elevated concentrations, to be transferred back to the neuron as its non-excitotoxic precursor glutamine. It is important to keep extracellular levels of neurotransmitters low in order to stop signaling at the synapse and allow for the signaling process to regenerate.

# The Glutamine / Glutamate Cycle

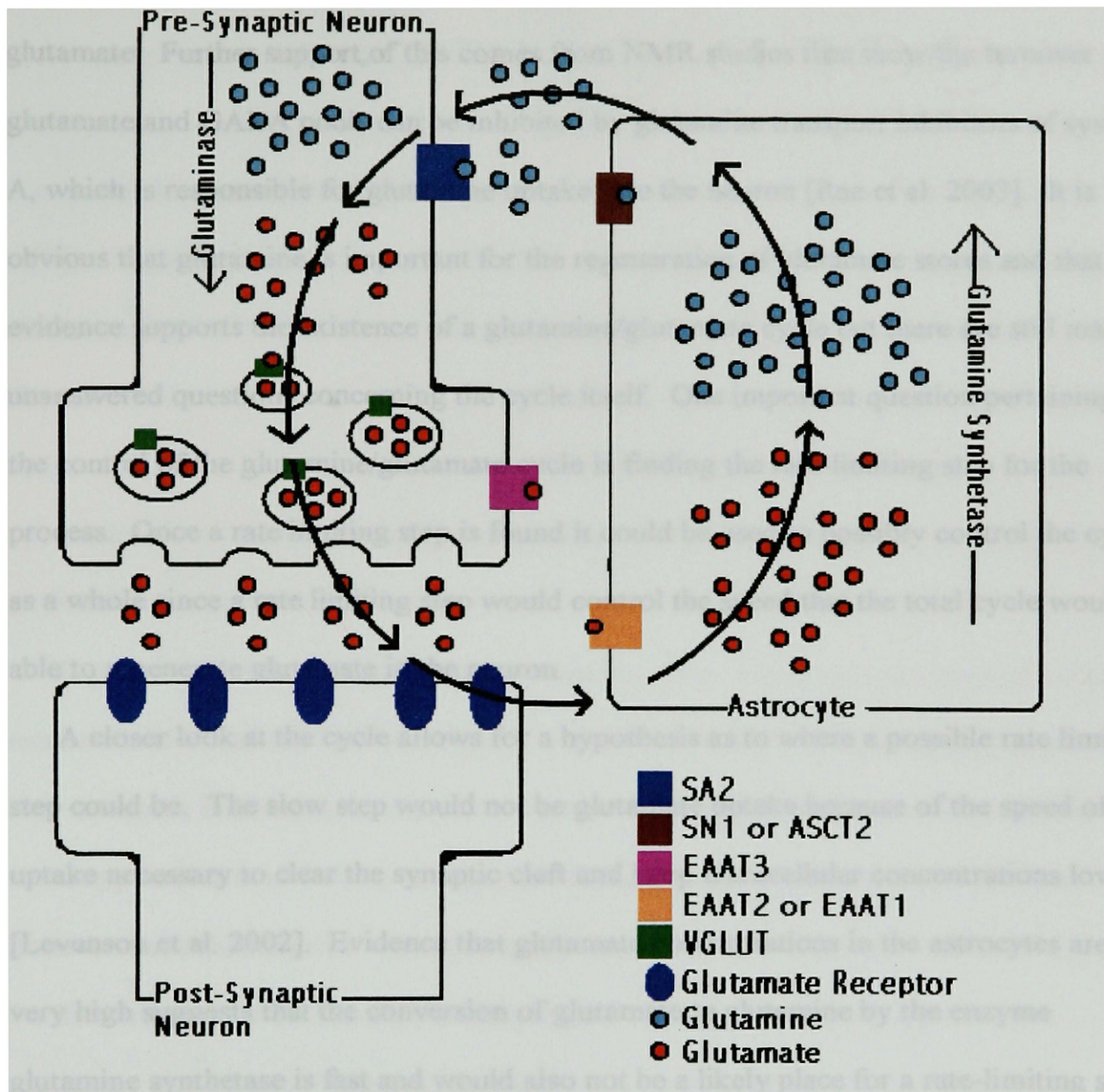


**Figure 1:** The glutamine-glutamate cycle converts glutamate to glutamine in the astrocyte and glutamine to glutamate in the neuron. This process allows glutamate supply in the neuron to be restored through the conversion of its non-excitotoxic precursor glutamine.

Evidence to support the glutamine/glutamate cycle has come from blocking the enzyme glutamine synthetase [Barnett et al. 2000] and inhibiting glutamine uptake into

neurons [Bacci et al. 2002]. Both studies demonstrated a depletion of glutamate in the neuron supporting that glutamine is necessary in order to maintain the supply of glutamate. Further support of this comes from NMR studies that show the turnover of glutamate and GABA pools can be inhibited by glutamine transport inhibitors of system A, which is responsible for glutamine uptake into the neuron [Rae et al. 2003]. It is obvious that glutamine is important for the regeneration of glutamate stores and that this evidence supports the existence of a glutamine/glutamate cycle but there are still many unanswered questions concerning the cycle itself. One important question pertaining to the control of the glutamine/glutamate cycle is finding the rate-limiting step for the process. Once a rate limiting step is found it could be used to possibly control the cycle as a whole since a rate limiting step would control the speed that the total cycle would be able to regenerate glutamate in the neuron.

A closer look at the cycle allows for a hypothesis as to where a possible rate limiting step could be. The slow step would not be glutamate uptake because of the speed of uptake necessary to clear the synaptic cleft and keep extracellular concentrations low [Levenson et al. 2002]. Evidence that glutamate concentrations in the astrocytes are not very high suggests that the conversion of glutamate to glutamine by the enzyme glutamine synthetase is fast and would also not be a likely place for a rate-limiting step. The options that remain are glutamine efflux from the astrocytes or uptake of glutamine into the neurons [Albrecht, 1989]. These two processes are supposedly controlled by system N and system A respectively (see Figure 1). This research concentrates on finding inhibitors for the SN1 transporter (system N).

Not only will specific inhibitors for the SN1 transporter allow determination of

whether it might be a target for control of the glutamine/glutamate cycle but these inhibitors will also facilitate the characterization of the SN1 transporter's activity profile. The research to date has built as follows. First, the SN1 transporter was predicted to preferentially interact with glutamine [Kilberg et al. 1980]. Second, the SN1 transporter is expressed in astrocytes where glutamine pools are also found [Nagaraja and Brookes, 1996]. Third, the SN1 transporter has been shown to localize to the plasma membrane of astrocytes and efflux glutamine under physiological conditions [Chaudhry et al. 1999]. Fourth, the SN1 transporter is the only transporter that has been identified to cause net amino acid efflux from astrocytes, the rest of the transporters require substrate on the opposing side of the membrane to exchange for glutamine [Bröer et al. 2002, Dietmer et al. 2003].

Even with the knowledge of the SN1 transporter to date some questions still need a more definitive answer. In the literature a discrepancy has arisen according to whether SN1 transport is electroneutral [Chaudhry et al. 1999] having no net charge flux, or electrogenic [Fei et al. 2000], having a net charge flux and thus producing a current. Some evidence is recorded with asparagine causing inward currents in oocytes expressing the SN1 transporter during depolarizing conditions that seems to suggest electrogenic transport. The proposal was that the transport process involved the uptake of two sodium ions and a neutral glutamine with the antiport of a proton and a net charge flux of +1 into the cell [Fei et al. 2000]. The opposing view was that the process was electroneutral with the uptake of a neutral glutamine and sodium cation with the antiport of a proton and no net charge flux for the process. One piece of evidence for this is that the  $K_m$ , or the affinity for substrate, for system A, which is electrogenic, varies with membrane potential

while the  $K_m$  for the SN1 transporter is not affected by membrane depolarization. It was later suggested that the transport process is demonstrating the behavior of both coupled and uncoupled proton conductance (see Figure 2) to satisfy the observations of both groups [Chaudhry et al. 2001].

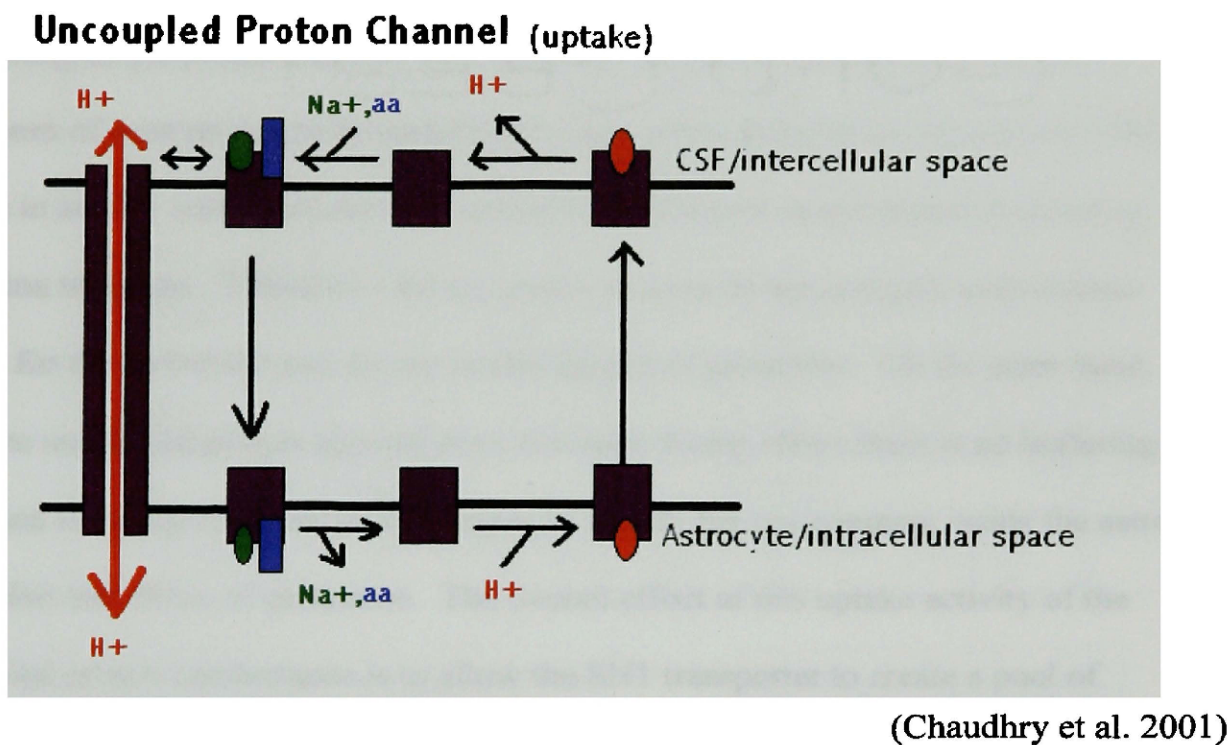


**Figure 2:** Illustration of the uncoupled proton channel that opens during glutamine uptake by the SN1 transporter.

The current proposed mechanism of action for the uncoupled proton channel model for uptake of glutamine by the SN1 transporter involves first the binding of glutamine and then the binding of a sodium cation [Bröer and Brooks, 2001]. As the complex crosses the membrane to the inside of the astrocyte a non-stoichiometric proton channel

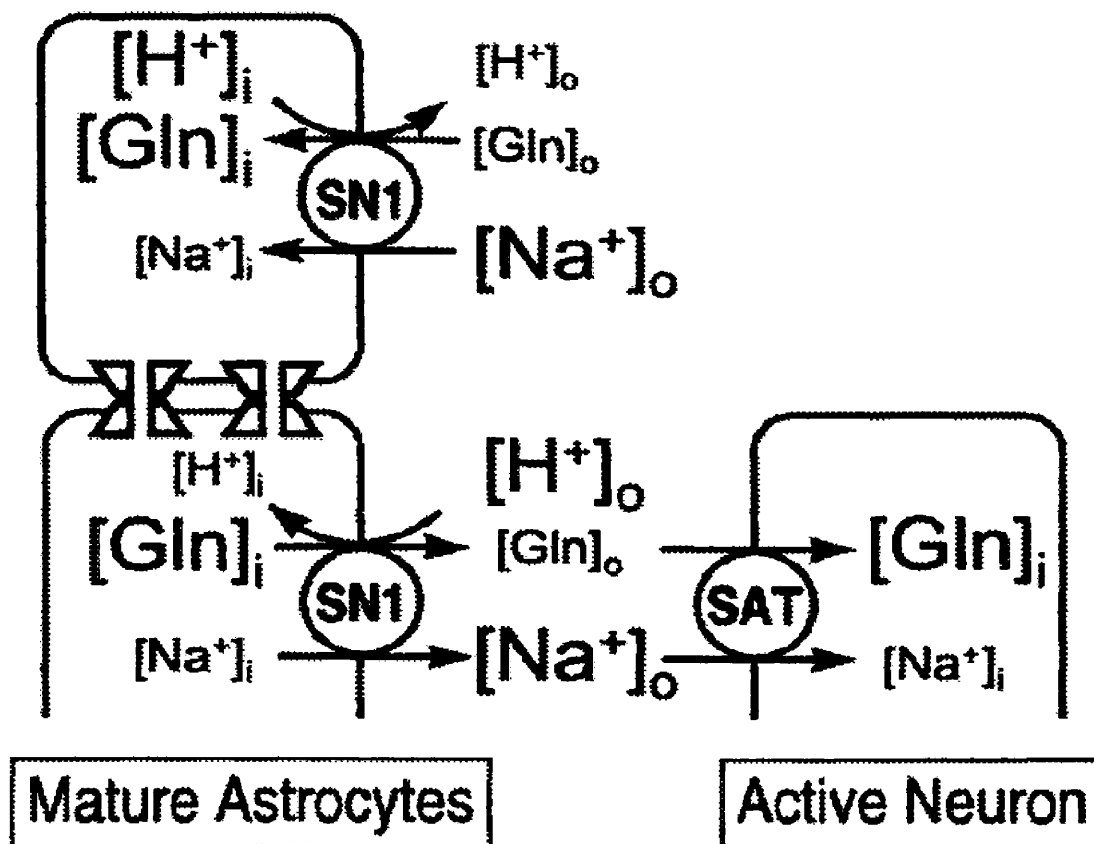


opens. The transporter releases the sodium cation and glutamine and then binds a proton and crosses the membrane to be released on the outside of the astrocyte, resetting the transporter to begin the process over again. The uncoupled proton channel does not open during glutamine efflux [Chaudhry et al. 2001].

The physiological significance of the opening of the uncoupled proton channel during uptake is interesting because the SN1 transporter is inhibited by low pH. During uptake the opening of the proton channel allows for the uncoupled (non-stoichiometric) movement of protons across the membrane. This uncoupled proton movement buffers the rise in acidity outside of the cell caused by the antiport of the proton involved in glutamine transport. Therefore, during uptake protons do not compete with sodium cations for the active site and do not inhibit uptake of glutamine. On the other hand, since the uncoupled proton channel does not open during efflux there is no buffering effect and the antiport of the proton begins to acidify the environment inside the astrocyte and inhibit the efflux of glutamine. The overall effect of this uptake activity of the uncoupled proton conductance is to allow the SN1 transporter to create a pool of glutamine inside the astrocyte and allow gradual efflux into the CSF [Bröer and Brookes, 2001][Chaudhry et al. 2001].

An interesting caveat of the SN1 transporter pharmacology profile is how it matches up against the profile for system A (Figure 3). In system A transport glutamine uptake is electrogenic and sodium dependent. The sodium cation and the glutamine efflux from the SN1 transporter would directly correlate with the sodium cation and glutamine uptake of system A transport. Also, system A transport is inhibited by low pH so the antiport of the proton by the efflux mechanism of SN1 would help keep system A transport from

being inhibited by low pH [Bröer and Brookes, 2001] [Chaudhry et al. 2001]. This matching of the two transport profiles could also point to the possibility that the SN1 transporter is the rate limiting step of the entire glutamine/glutamate cycle.



(Bröer et al. 2001)

**Figure 3:** This figure demonstrates the different flux situations for the SN1 transporter and the interesting synergy of the efflux by the SN1 transporter and the uptake of system A transport. The SN1 transporter uptake is represented by the upper portion of the astrocyte while SN1 efflux is represented by the lower portion of the astrocyte. The larger type implies larger concentrations and vice versa. The subscripts i and o refer respectively, to intracellular and extracellular concentrations.

Another aspect of system N, not the SN1 transporter specifically, that is very interesting is that there is an as yet unidentified sodium independent transporter that is

considered to be responsible for the majority of glutamine transport at the blood brain barrier [Deitmer et al. 2003] [Bröer and Brookes, 2001]. This transporter could be a novel target for drug delivery.

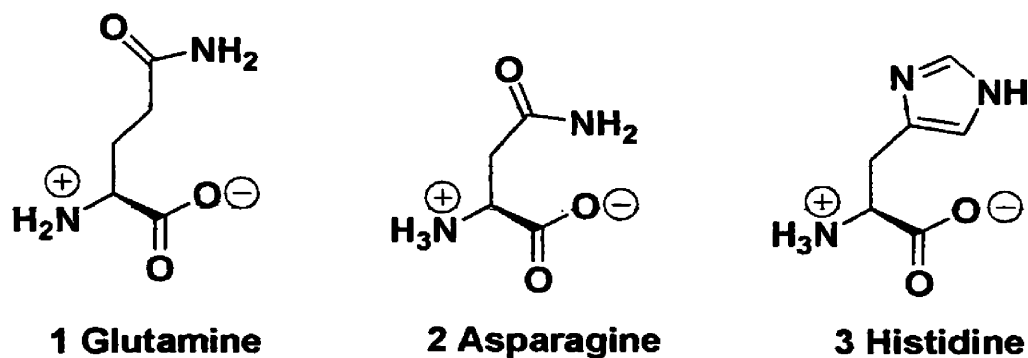


**Figure 4:** The three natural substrates transported by SN1; glutamine 1, asparagine 2, and histidine 3.

Analysis of the three natural amino acid substrates recognized by the SN1 transporter (glutamine 1, asparagine 2, histidine 3) frames a rudimentary concept of what the initial binding site map (Figure 5) might entail. A chiral interaction involving the ammonium and carboxylate functionalities should be important since the D-amino acids are not substrates. A hydrogen bonding interaction, accepting and/or donating, at the distal end of the amino acid is a property that all three amino acids share. Through building and testing asparagine analogues with aryl amine pendant groups, information will become available about the space in the binding site for tolerating the bulk of those substituents, some directional preferences based on conformational energies, and binding interactions with the binding site based on substituents properties.

## Initial SN1 Transporter Binding Site Map

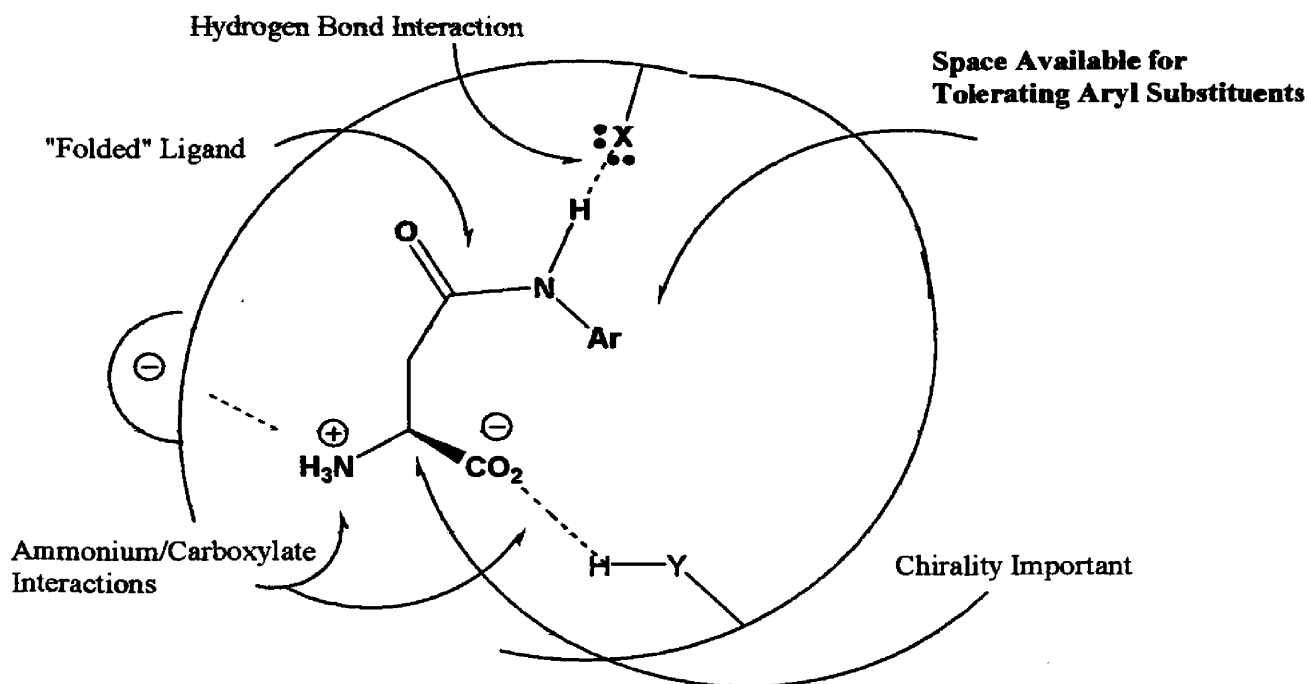


**Figure 5:** The initial SN1 transporter binding site map incorporates the “folded” conformation for the analogues and three electronic interactions. This map is preliminary and through the testing of the proposed analogues a more detailed map will be made.

The target analogues involved with this project are asparagine length and have large aromatic pendant groups on the asparagine amide functionality (see Figure 6). The concept for these analogues comes from previous research involving glutamine analogues that inhibit glutamine uptake by the SN1 transporter [Ripley 2005] (Figure 6).

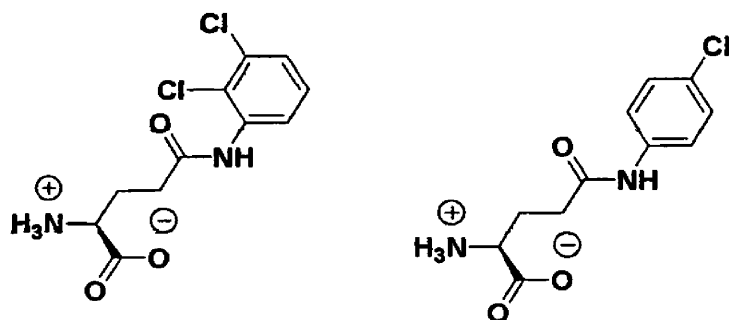


**Figure 6:** N-aryl glutamine analogues.

The asparagine analogues are to be synthesized and assayed against the SN1 transporter expressed in oocytes, or unfertilized frog eggs from *Xenopus laevis*, for ability to inhibit glutamine uptake. Using the results of the assays to create structure/activity relationships, improvements will be made on the initial binding site map above. With more information about ligand-protein binding interactions, more potent inhibitors can be specifically designed and help determine whether the SN1 transporter is a good target for regulation of the glutamine/glutamate cycle.

**The target asparagine analogues**

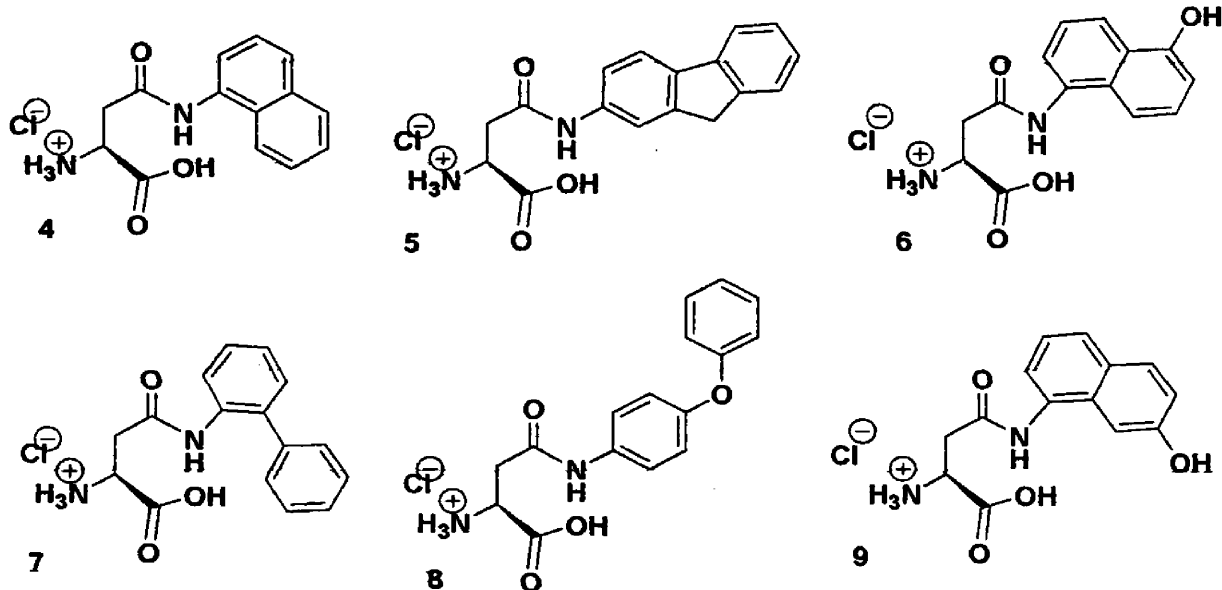


**Figure 7:** The family of asparagine analogues to be synthesized. All of these analogues will probe the space allowed in the binding site but 6 and 9 also incorporate hydroxyl groups that will look for possible hydrogen bond acceptors near the binding site that might facilitate binding.

The target analogues will all have the L-specific configuration and vary from each other only by the aromatic system attached (Figure 6). The amides 4, 5, 7, and 8 will specifically probe the space in the binding site as well as any hydrophobic pockets that

could facilitate the binding of a ligand. The amides **6** and **9** will probe the same space for possible hydrogen bond accepting moieties. An additional reason for probing the space tolerated in the binding site is that if these larger groups are tolerated then analogues with fluorescent groups, covalent modifier groups and positron emission tomography (PET) tags (Figure 7) could be tolerated as well. These compounds would allow for fluorescence, covalent modification and PET studies to further elucidate the characteristics of the SN1 transporter such as detailed mechanism of transport kinetics, location of the transporter, and requirements for inhibition of the SN1 transporter.

### Future directions

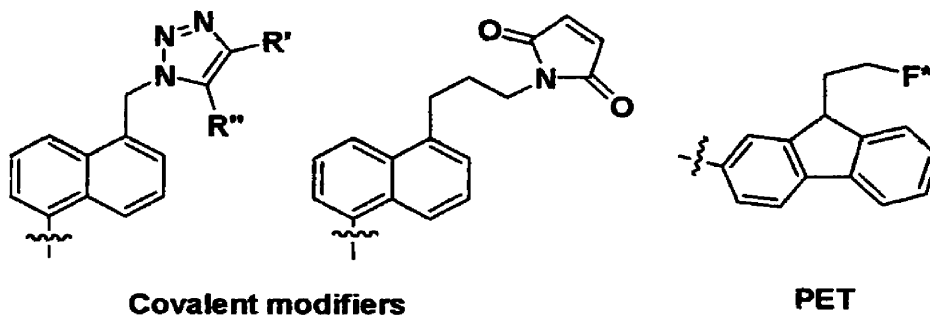
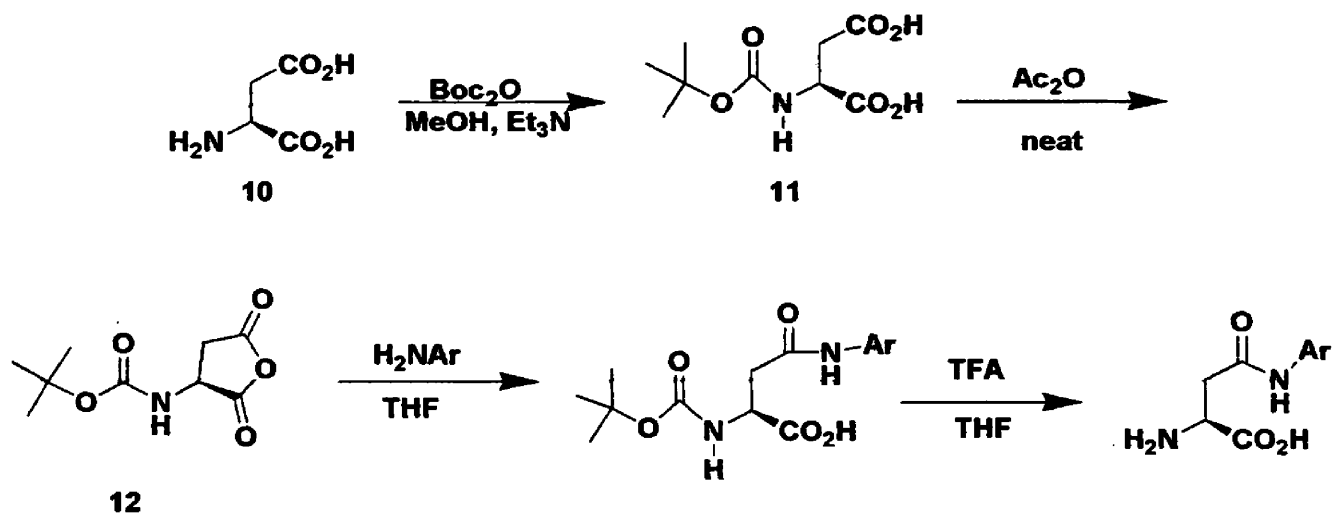


**Figure 8:** Two possible covalent modifier groups are shown on the left. The furthest left would be photo activated while the other would be thiol activated. The PET tag is shown on the right.

## Discussion:

The original synthetic route to targets 4-9 involved protection of aspartic acid 10 as the *tert*-butyl carbamate (Boc-aspartic acid) 11 and then formation of the anhydride 12 (Scheme 1). The anhydride was reacted with the aryl amines to produce the amide. The carbamate could then be cleaved under acidic conditions (trifluoroacetic acid, TFA) to afford the targets 4-9. 1-Naphthylamine was chosen as the model aryl amine with the idea that once the synthetic route had been taken to target 4 then targets 5-9 would be obtained.

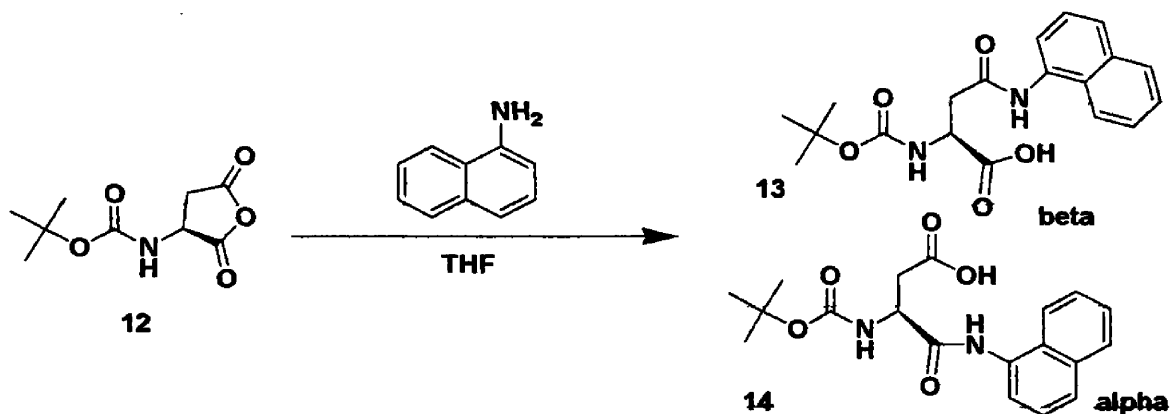


**Scheme 1:** The protection of the L-aspartic acid 10 using di-*tert*-butoxycarbonyl anhydride (Boc<sub>2</sub>O) to produce the carbamate 11. The carbamate was then reacted with acetic anhydride to make the anhydride 12. The anhydride was then combined with an aryl amine and then deprotected using trifluoroacetic acid (TFA).

The anhydride 12 readily decomposes back to the di-acid 11 if it comes in contact with any water. Therefore, the anhydride 12 is exceedingly hard to store and one of the

downfalls of this synthetic route [Yang and Su, 1986]. Because of its instability, the anhydride **12** was made prior to each addition reaction and then carried on through the addition immediately after workup to minimize degradation.

Another downfall of this reaction was that the beta addition product **13** was contaminated with the alpha addition product **14** that also happened to be the major product for the reaction (Scheme 2).



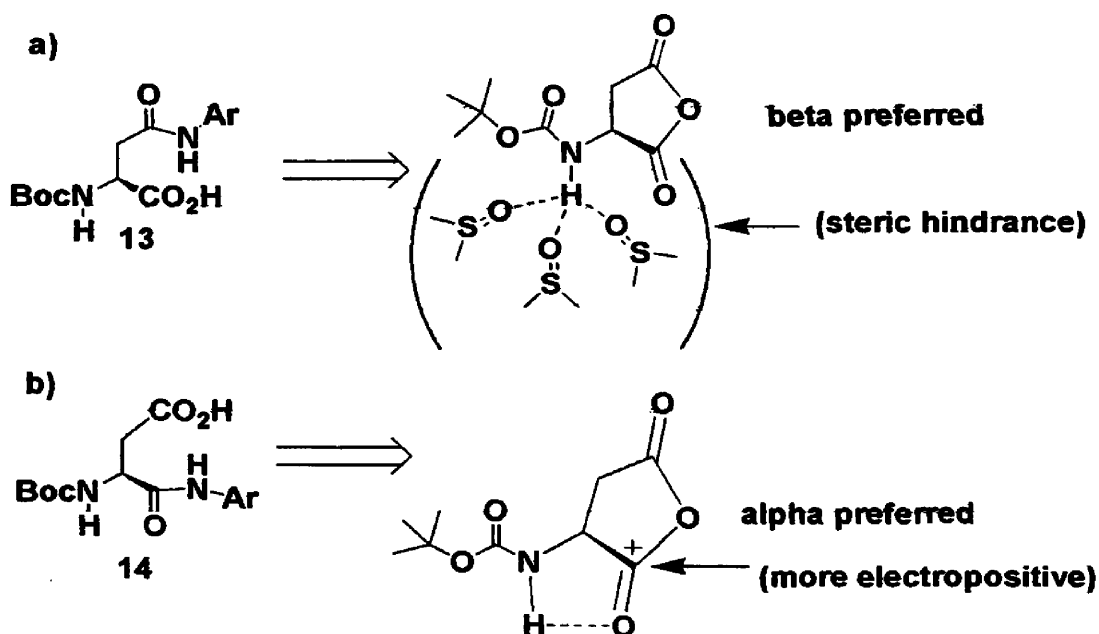
**Scheme 2:** The reaction of the anhydride **12** with naphthylamine produces both a beta **13** and an alpha **14** product.

These two compounds are very difficult to separate from each other efficiently using silica chromatography because of the intermolecular affinity between the aromatic ring systems. The aromatic rings increase the difficulty of the separation considerably by causing a situation where the two very similar compounds “ride” each other. Addition product **14** elutes before addition product **13** but in a manner that the overlap affords very small fractions of pure **13** or **14** and mostly a mixture of the two addition products. Toluene was added to the mobile phase used for TLC in an attempt to disrupt the affinity that addition products **13** and **14** might have for each other but no difference in separation was observed. Also, addition product **14** is the major product in any solvent system other



than DMF (dimethylformamide) and DMSO (dimethylsulfoxide) [Yang and Su, 1986]. DMSO and DMF are notoriously difficult to get away from reaction products and therefore not a desirable reaction solvent option. Since the major product for the reaction is addition product **14** this also increases the difficulty of achieving a pure fraction of addition product **13**. The elution situation is best thought of as the overlap of two Gaussian peaks that maintain a similar difference between maxima but the existence of a much larger peak for the addition product **14** tends to overlap severely with the smaller peak for addition product **13**. Therefore, the solvent system for silica separations that is effective tends to border on the lower end of solubility for the two addition products.

The mechanism of preference for **14** involves an intramolecular hydrogen bond formation in the form of a five-membered ring [Albini et al. 1985] that increases the partial positive charge on the alpha carbonyl therefore making it more susceptible to attack by the aromatic amine (Figure 8).

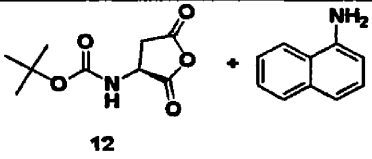
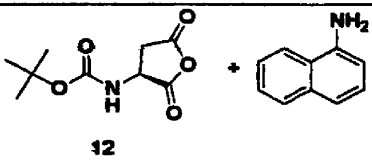
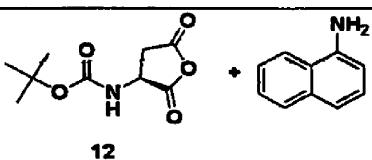
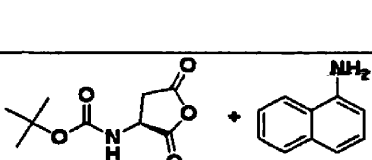
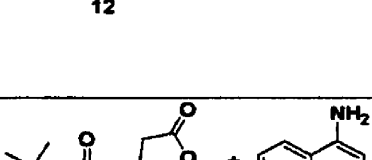
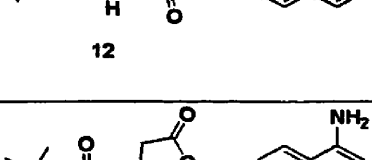


(Yang and Su, 1986)

**Figure 9:** a) The beta product 13 is preferred when the carbamate hydrogen is hydrogen bonding to the solvent. b) The alpha product 14 is preferred when the carbamate hydrogen is involved in an intramolecular hydrogen bond that makes the alpha carbonyl more electropositive.

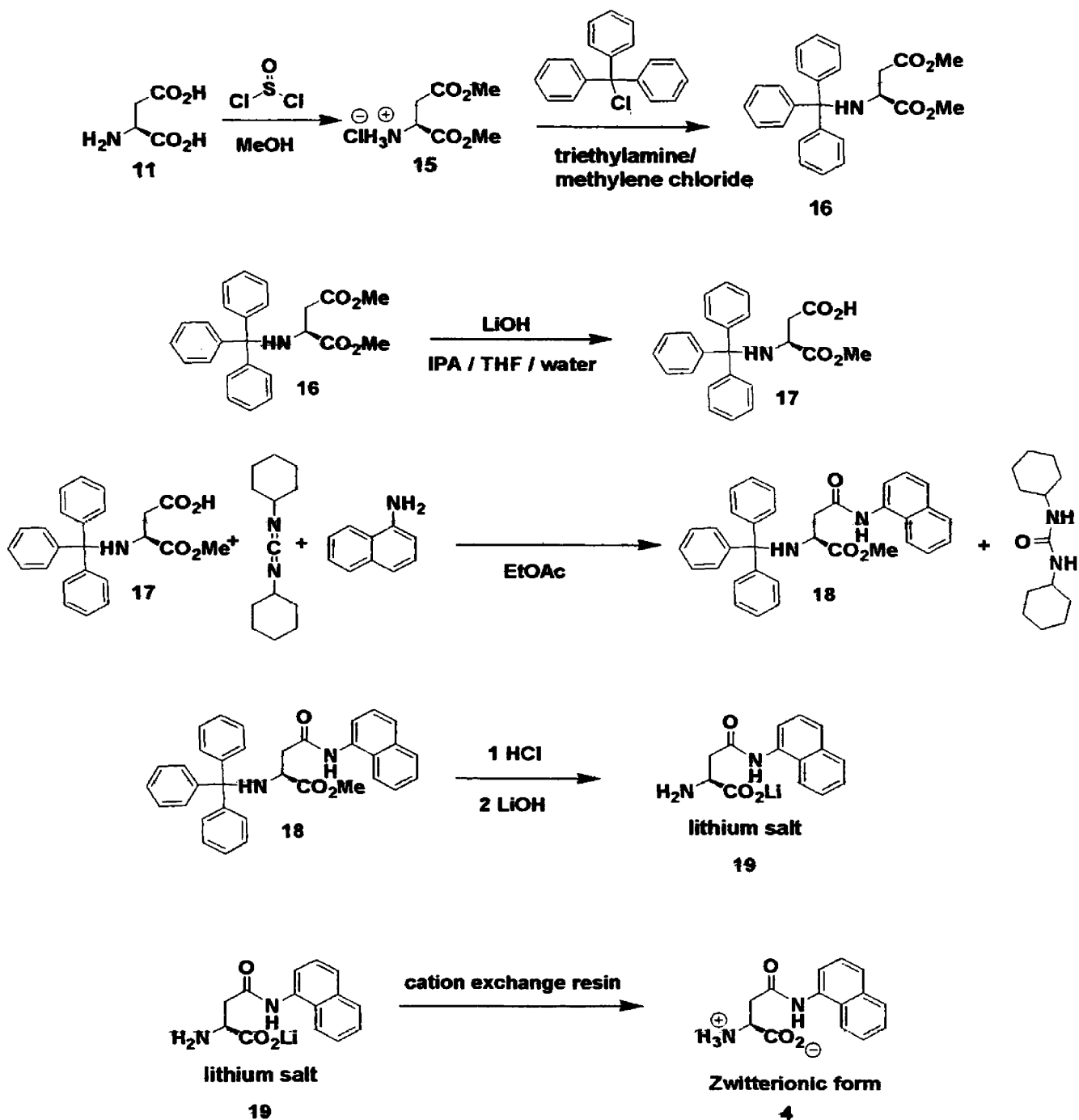
Solvents with high polarity, such as DMSO, act as hydrogen bond acceptors and break the stability of the five-membered ring hydrogen bond situation and create a steric situation around the proximal or alpha carbonyl. Breaking the hydrogen bond makes both the alpha and beta positions equally susceptible, electronically, for attack by the amine. The space around the alpha position also becomes crowded by the solvation of the amide hydrogen and therefore addition at the distal or beta carbonyl may be favored (Figure 8) [Yang and Su, 1986]. Pyridine was added to the reaction to try and break the proposed hydrogen bond formation but no difference in 13/14 ratio was observed.

TLC identified the addition products **13** and **14** to have green and red stains, respectively, with ninhydrin. Identification was achieved by comparing a reaction carried out in DMSO (favoring **13**) and a reaction in ethyl acetate (favoring **14**) and using ninhydrin. Then a series of reactions using diethyl ether, 50/50 diethyl ether/THF, 50/50 diethyl ether/ methylene chloride, THF (tetrahydrofuran), acetonitrile and DMSO as solvents revealed that THF might create a situation where the **13/14** ratio was such that chromatography might be a viable option when compared to the difficulty of working with solvents like DMSO and DMF (Table 1). Only THF (Entry 4 on Table 1) seemed to give a ratio of **13/14** that would be viable for silica separations. The difference between DMSO (Entry 6 on Table 1) and the other solvent situations was drastic. Pyridine was added to the same set of reactions in an attempt to break up the activation of the alpha carbonyl and increase the **13/14** ratio but the reactions still yielded too little of the beta product to make the synthesis viable for recovery of the desired product. THF seemed to be the best option out of the solvent situations other than DMSO and DMF but even then the ratio was estimated to be about 20/80 of **13/14** as determined by HPLC.

Entry	Reactants	Conditions	13/14 ratio (observed by TLC)
1	 12	diethyl ether	small
2	 12	50/50 diethyl ether/THF	small
3	 12	50/50 diethyl ether/methylene chloride	small
4	 12	THF	More 14 than 13 but better than other conditions
5	 12	acetonitrile	small
6	 12	DMSO	Large (very little alpha observed)

**Table 1:** The results of six different solvent situations that were tried in order to see if the beta/ alpha 13/14 ratio could be improved.

The next alternative was to pursue a reaction scheme that would allow selective addition at the distal carbonyl and thereby sidestep the separation of **13/14** beta/alpha mixtures. A reaction scheme (Scheme 3) creating the dimethyl ester of aspartic acid and then using trityl protection to create conditions to selectively deprotect the distal methyl ester was conceived. The distal carboxylic acid would then be reacted with dicyclohexylcarbodiimide (DCC) to couple the acid and the aryl amine [Klausner and Bodansky, 1972].

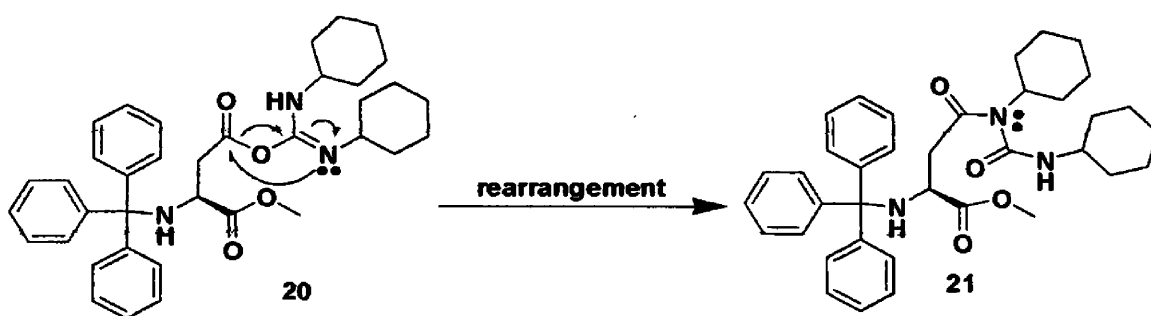


**Scheme 3:** Reaction scheme that uses the trityl protecting group to create a steric situation that allows the mono deprotection of a dimethyl ester of aspartic acid. The mono-acid is then used in a coupling reaction with DCC and naphthylamine to achieve only the beta or 18 adduct.

L-aspartic acid 10 is easily converted to di-ester 15 in quantitative yields. The trityl protection to produce 16 is also done with ease. The trityl protection creates a steric

situation where the alpha ester is effectively blocked by the bulk of the aromatic rings creating a situation where only the beta ester is cleaved to produce the mono-acid **17**. The mono-acid product **17** can then be selectively coupled with the aryl amine in the presence of dicyclohexylcarbodiimide (DCC) to produce the amide **18**. Since only the amide **18** is created, chromatography to separate beta and alpha products is no longer necessary. The trityl group is easily cleaved under acidic conditions which could then be followed by a simple hydrolysis of the methyl ester to afford the lithium salt **19**. The target **4** could then be obtained by use of a cation exchange resin.

The first attempts to produce the amide **18** seemed to suggest that it might actually precipitate from ethyl acetate and hexanes greatly simplifying purification since the aryl amine, in this case naphthylamine, is readily soluble in the mixture of the two solvents. There was considerable difficulty reproducing the initial reaction as far as getting the mono-acid **17** to disappear (react completely) and isolating amide **18** again through precipitation. Attempts to separate the product chromatographically have shown that the TLC spot previously thought to be the desired product is actually the DCC-**17** adduct **20** [Klausner and Bodansky, 1972] (Scheme 4).



(Klausner and Bodansky, 1972)

**Scheme 4:** The activated ester **20** can rearrange to the inactive adduct **21**.

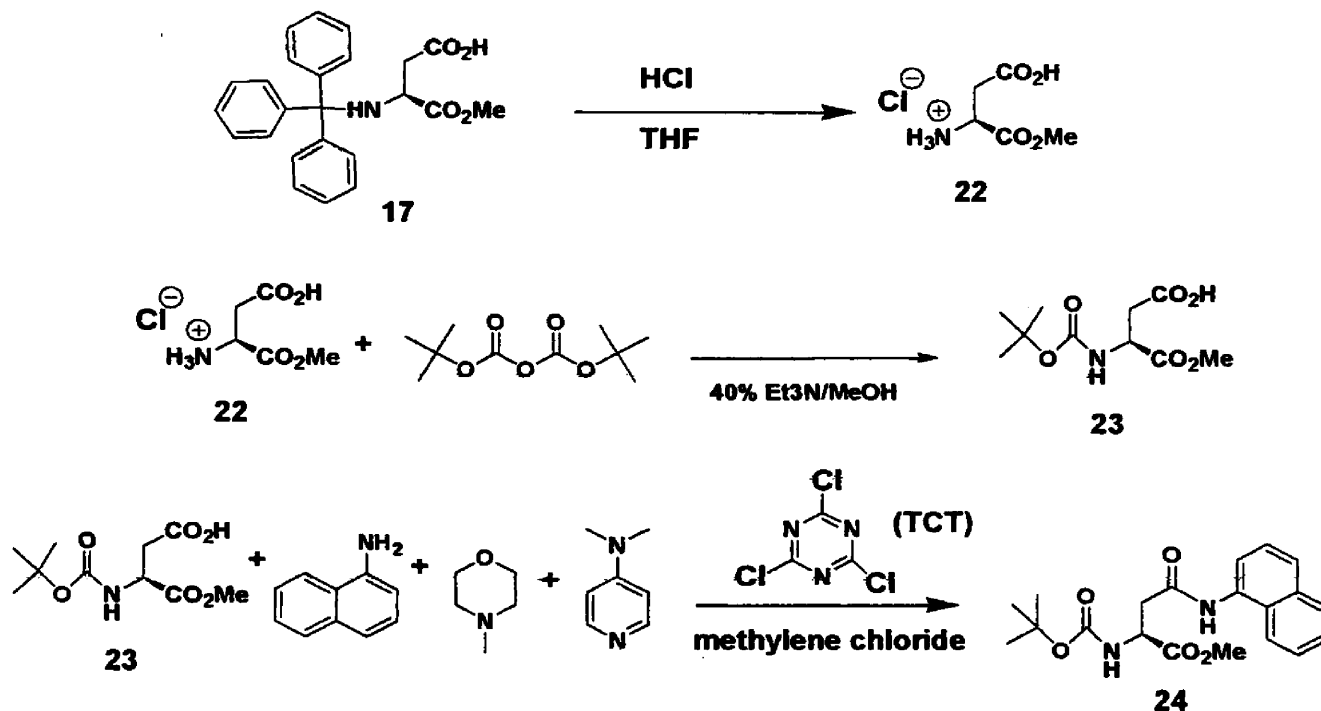
So the product thought to be **18** observed by NMR could have been a result of naphthylamine, mono-acid **17**, and the DCC adduct **20** all included in the hexane/ethyl acetate precipitation. All subsequent attempts to synthesize the amide **18** resulted in products with NMR spectra that lacked signals in the naphthyl region and contained signals indicative of the cyclohexyl groups that would be expected for the adduct **20**. (cti080904p98\_1) (NMR attached p58) Scheme 4 shows the rearrangement of intermediate **20** to unreactive adduct **21** that could be responsible for this result. [Klausner and Bodansky, 1972] A reaction was allowed to proceed for three days and finally the green ninhydrin stain indicative of the amide **18** was observed by TLC. DMF was added to try increasing the nucleophilicity of naphthylamine and improve the reaction speed but no noticeable improvement was observed.

At first it was thought that steric issues between the trityl group and the cyclohexyl groups of DCC might be causing problems, but several reactions were attempted using diisopropylcarbodiimide (a coupling reagent that contains isopropyl groups instead of cyclohexyl groups and therefore less bulky) and the results were similarly disappointing. The only explanation remaining was that naphthylamine was not nucleophilic enough to displace the carbodiimide at the distal carbonyl. The best course of action was to remove the trityl group and replace it with a Boc group that could survive the acid chloride formation on the distal carboxylic acid to compensate for the nucleophilicity of the aryl amines.

The replacement of the trityl group of mono-acid **17** was simple as was the protection using  $\text{Boc}_2\text{O}$  to make the mono-acid **23**. The cyanuric chloride (TCT) reaction to create

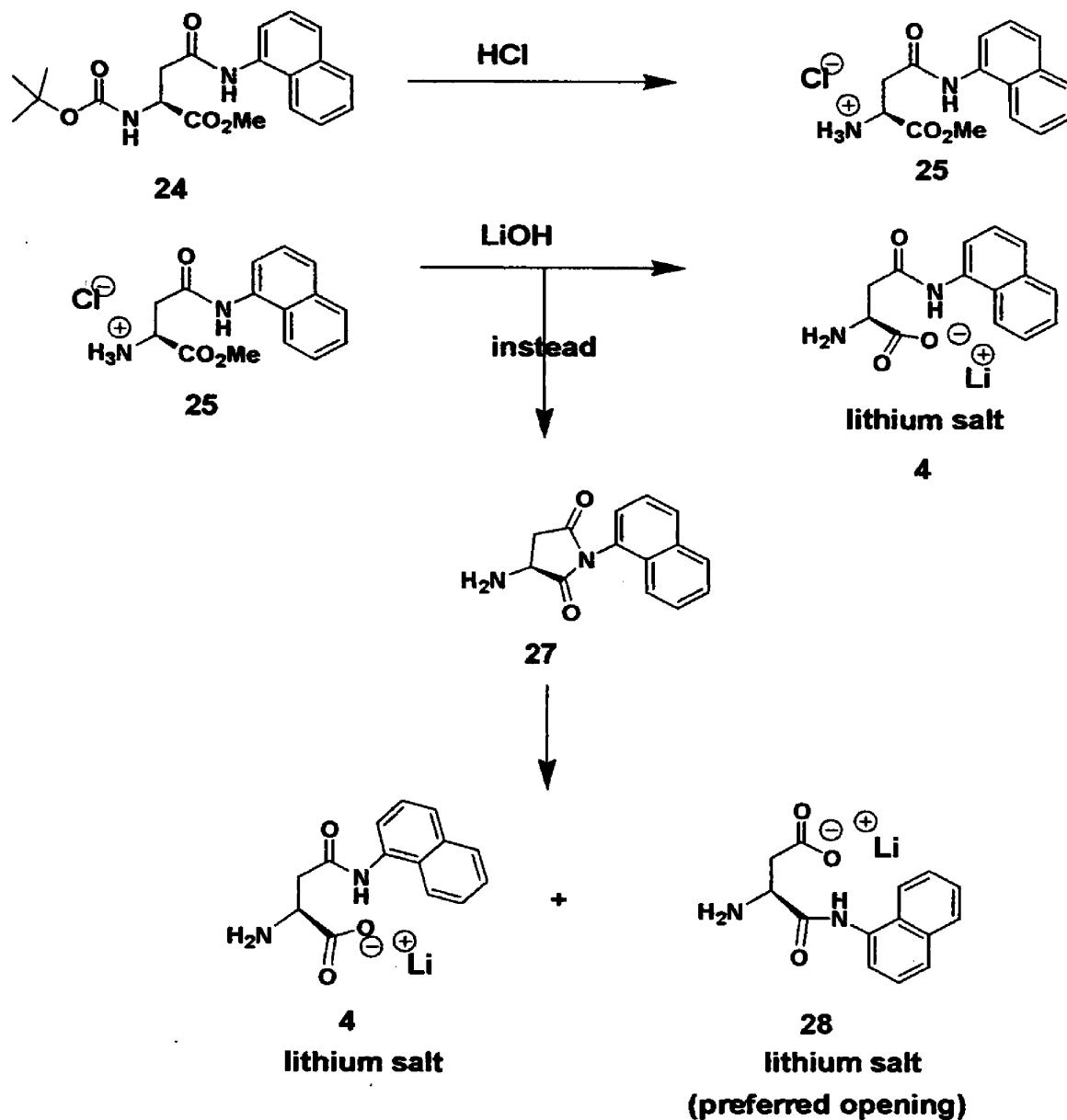


the acid chloride in situ went to completion much faster than the DCC coupling and involved a comparably easy workup to produce pure amide **24** (Scheme 5).



**Scheme 5:** The trityl deprotection of the mono-acid **17** using acid and the re-protection of mono-acid **22** using **Boc<sub>2</sub>O** allowed for the much harsher in situ generation of the acid chloride by **TCT** to achieve amide **24**.

The cleavage of the **Boc** group of amide **24** with **HCl** worked fine but there were problems with the hydrolysis of the methyl ester to produce target **4** (Scheme 6). While monitoring the hydrolysis step of ester **25** by TLC with 10% methanol/methylene chloride, the stain for the alpha amide **28** appeared. The basic hydrolysis of the methyl ester **25** creates a situation where an intramolecular ring closing occurs to form the five-membered ring **27**. The five-membered ring **27** then opens as the either amide **28** or beta amide **4** [Greenfield et al. 2005].



**Scheme 6:** The cleavage of the Boc group of amide **24** with HCl afforded ester **25**. The problem arises during basic hydrolysis of the ester **25** when the intermediate **27** is formed and reopens as a mixture of the target **4** and amide **28**.

This observation had also been made in work that used NaOH instead of LiOH and it was thought that with the weaker base the problem might be evaded. The previous investigator found the hydrolysis problem and circumvented it by using a benzyl group to protect the proximal carboxylic acid because it could be removed through hydrogenolysis

at elevated pressure and those conditions did not degrade the product [Greenfield et al. 2005] (Figure 9). However, the work did not mention the synthetic route to achieve the selectively deprotected benzyl ester intermediate.

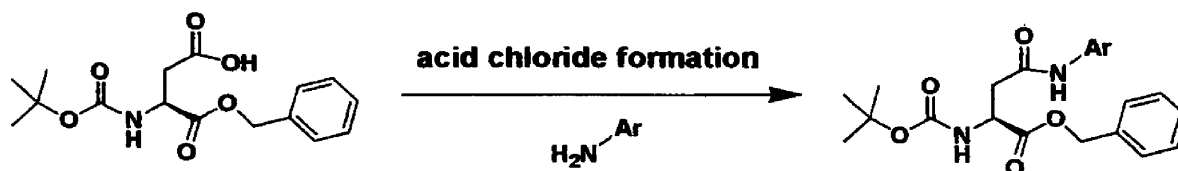
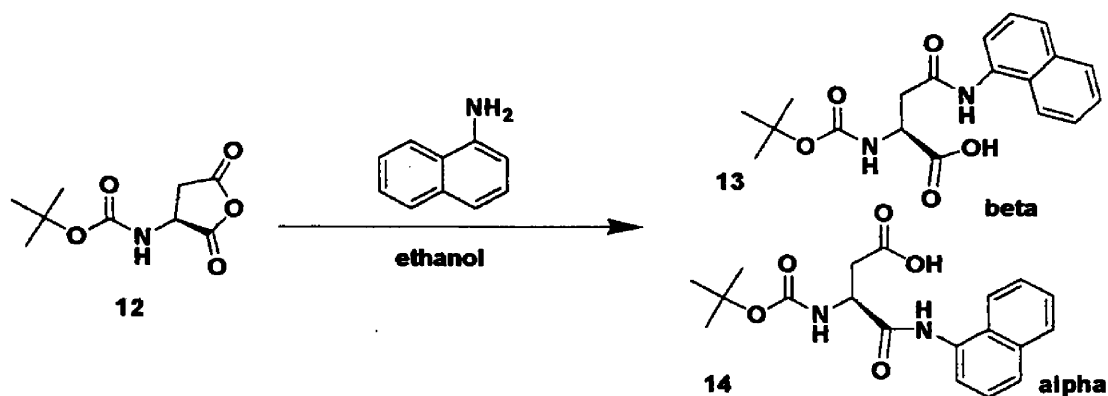


**Figure 10:** The alpha-O-benzyl mono protected Boc-L-aspartamide (above) could be used instead of ester 24. The benzyl ester can be deprotected using hydrogen and a catalyst without going through the intermediate 27 [Greenfield et al. 2005].

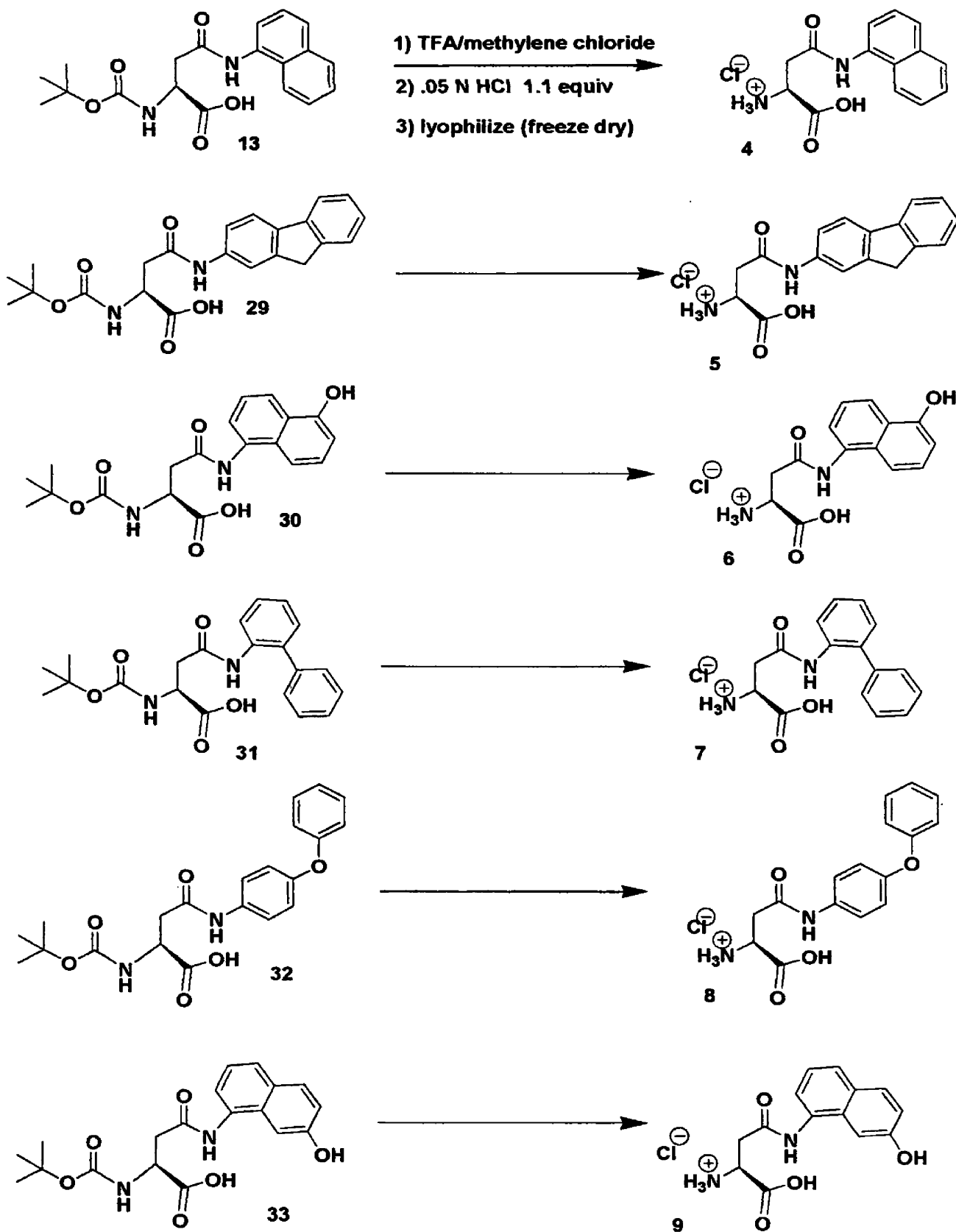
The contamination of target 4 with amide 28 (beta with alpha) completed a multi-step synthesis only to be faced with the same problem posed by the aspartic anhydride route in quite a few less steps. For the sake of actually getting product to the final stage it was decided to return to the original aspartic anhydride synthetic route with the hopes that enough of the pure beta of each compound could be isolated and then deprotected to achieve the final targets 4-9.

It was realized that the use of ethanol or methanol allowed for a 13/14 ratio of about 50% (Scheme 7) which would be much better than the 20/80 beta/alpha ratio that was found using THF as the solvent [Yang and Su, 1986]. Through optimizing the separations for this reaction it should be possible to get enough of the beta products to carry on through deprotection.



**Scheme 7:** Aspartic anhydride reaction with naphthylamine using ethanol as the solvent affords a much better **13/14** ratio.

The beta/ alpha ratios for the reactions with ethanol were much better than those for the THF reactions. The chromatography steps were slightly different from each other to achieve the pure beta addition product for each target compound but all of the beta compounds could be isolated using silica chromatography. The Boc group was cleaved using TFA in methylene chloride (Scheme 8). The TFA salts were then taken up in 1.1 equivalents of a .05 N solution of HCl. The solid was broken up in the solution and then the solution was frozen and lyophilized (freeze dried) to produce the HCl salts of the target asparagine analogues.



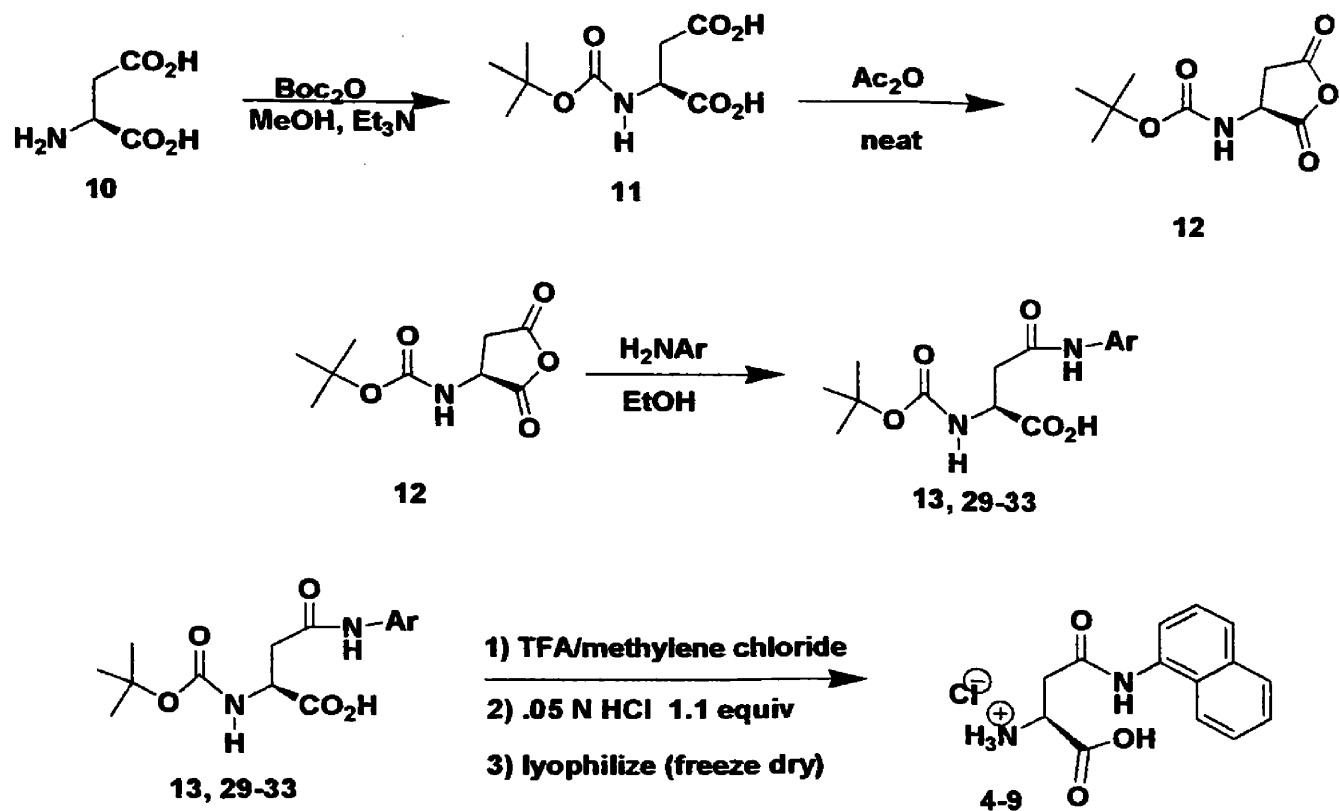
**Scheme 8:** The cleavage of the Boc group was achieved using TFA in methylene chloride. The TFA salt was then taken up in a .05 N HCl solution, frozen and then lyophilized.

## **Conclusion:**

The aromatic asparagine targets **4-9** have been synthesized and await biological testing. Based on previous results of aromatic glutamine analogues exhibiting glutamine uptake inhibition at the SN1 transporter [Ripley 2005] it is very likely that this set of compounds will show interesting biological properties. These results will aid in building a more accurate binding site map for the SN1 transporter. A more detailed binding site map will facilitate the design of more potent and selective inhibitors for the SN1 transporter.

The analogue design was chosen for the availability of further manipulation that will offer additional details of binding and transport mechanisms. These future analogues will contain, for example, fluorescent groups, covalently modifying groups and positron emitting groups. Using these modified analogues more sophisticated experiments can be performed offering finer detail for the transport process.

The current synthetic route (Scheme 9), although affords the target compounds, could be improved upon. Testing the hypothesis that the intramolecular hydrogen bond activation of the alpha carbonyl of anhydride **12**, a protection scheme eliminating the hydrogen and thus eliminating alpha carbonyl activation while concurrently hindering nucleophilic approach to the alpha carbonyl should afford predominantly the desired beta amides (Figure 10). This synthetic modification should afford higher yields of the beta amides.



**Scheme 9:** The synthetic route developed for aromatic asparagine analogues 4-9.

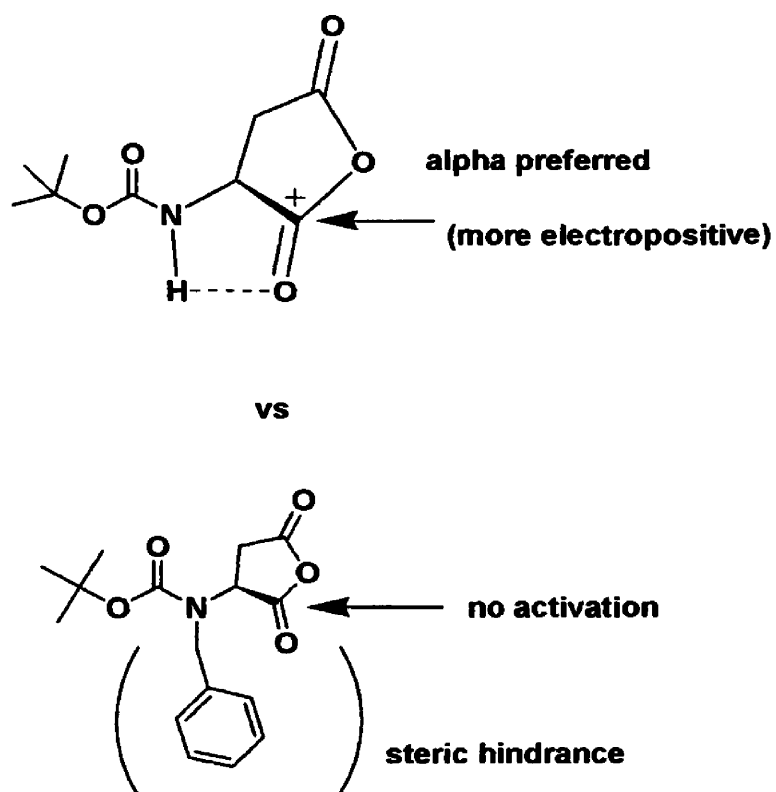
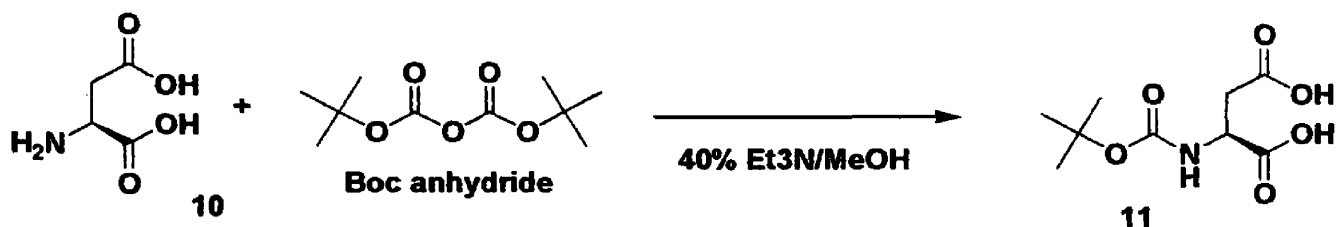


**Figure 11:** Synthetic modification to improve to improve yields for beta amides.

## **Experimental:**

Proton NMR was performed on a Varian 400 MHz with internal standard as chloroform<sub>d</sub> at 7.25ppm and DMSO<sub>d</sub> at 2.49 both relative to TMS in proton spectra or using preset parameters in D2O with acetonitrile as the standard at 1.93 ppm relative to TMS in proton spectra. Solvents were obtained from Mallincrodt, J.T. Baker and Fischer Scientific and used as is.

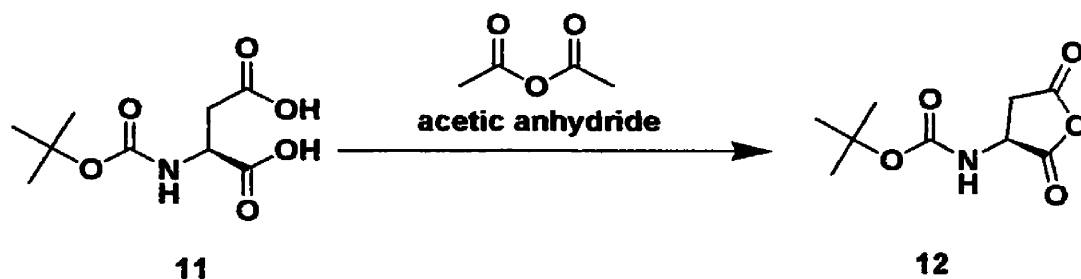




L-aspartic acid **10** (29.2 grams, 220 mmol) was stirred in a cold (ice bath) solution of 40% triethylamine (100 ml, 718.3 mmol, 3.26 eq) / methanol (150 ml). Boc anhydride (52.7g, 242 mmol, 1.1 eq) was added to the cold solution and the reaction was allowed to warm to r.t. and run for 24 hours. After satisfactory progress was observed through TLC then the pH was checked to see if still basic before evaporating under vacuum. Water (300 ml) was added and then extracted with diethyl ether (2x100 ml). The water fraction was kept and combined with ethyl acetate (300 ml). The pH was then adjusted around 2 using a 1M HCl solution and litmus paper. Sodium chloride was added to biphasic system to chase organics out of water layer. The ethyl acetate was then collected and the water solution was extracted again with ethyl acetate (100 ml and 200 ml consecutively). Ethyl acetate solutions were combined, dried over magnesium sulfate, and then evaporated to dryness under vacuum. The slightly yellow oil was then chased with washes of methylene chloride that were evaporated under vacuum as well. The solid was then put on a high vacuum pump and then ground in a mortar with pestle and then placed on the high vacuum again. The reaction made 44.5 g of Boc protected L- aspartic acid **11**, an 86.8% yield.

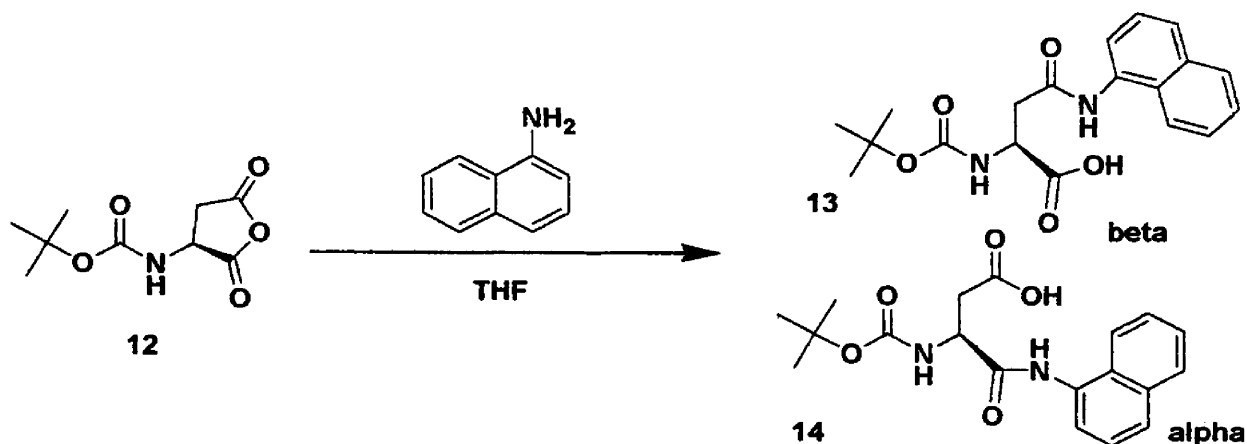
Cti071905p60\_4

**<sup>1</sup>H-NMR (400 MHz, CDCl<sub>3</sub>) ppm 6.95 (d, 1H, J=8.7Hz) ppm 5.63 (d, 1H, J=8.7Hz) ppm 4.65 (m, 1H)  
ppm 3.15 (dd, 1H, J=3.7Hz, J=17.1Hz) ppm 2.89 (dd, 1H, J=4.5Hz, J=17.8Hz) ppm 1.46 (s, 9H)**



Boc protected L-aspartic acid **11** (2.04 grams, 8.74 mmol) was added to acetic anhydride (20 ml, 212 mmol, 24.5 eq) and stirred at r.t. for 3.5 hours. Diethyl ether (40 ml) was then added to the reaction and the solution was decanted through filter paper and then evaporated to dryness under vacuum. The solid was washed with toluene and hexanes (2x each) to produce 1.76 g of a white solid, Boc L-aspartic acid anhydride **12**, a 93.3% yield.

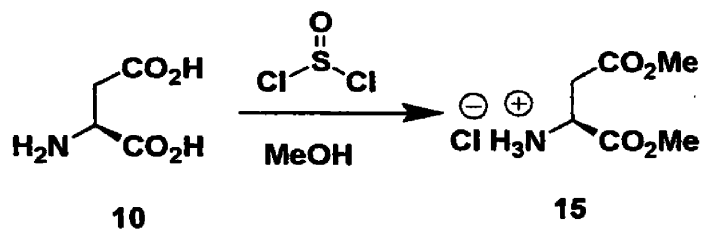
No NMR File (identified by TLC and then taken on immediately to the addition reactions)



Boc L-aspartic acid anhydride **12** (4.17 grams, 19.4 mmol) was reacted with  $\alpha$ -naphthylamine (2.23 grams, 15.5 mmol, .8 eq) in THF (30 ml) at r.t. for 24 hours. The reaction was then evaporated to dryness under vacuum to produce a purple solid. A silica column (100-150 ml) was performed using 1% acetic acid, 5% methanol, and 94% methylene chloride as the mobile phase to produce .267 g (.674 mmol, 4.5% yield) of the desired  $\beta$ -addition product **13** and 5.79 g of an  $\alpha/\beta$  mixture **13** and **14**.

Cti071205p52\_naphbocLasp

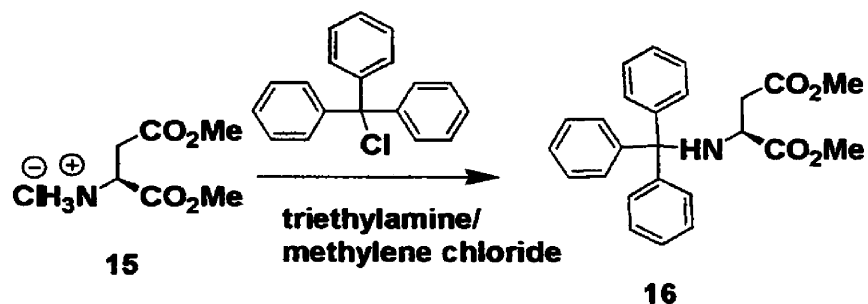
<sup>1</sup>H-NMR (400 MHz, CDCl<sub>3</sub>) ppm 8.20 (s, 1H) ppm 7.83 (d, 2H, J=5.8Hz) ppm 7.70 (d, 1H, J=6.7Hz) ppm 7.48 (d, 2H, J=4.6Hz) ppm 7.40 (s, 1H) ppm 5.97 (s, 1H) ppm 4.61 (s, 1H) ppm 3.29 (s, 1H) ppm 3.07 (s, 1H) ppm 2.86 (d, 1H, J=17.4Hz) ppm 2.53 (d, 1H, J=18.0Hz) ppm 1.45 (s, 9H)



L-aspartic acid **10** (20.9 g, 157.2 mmol) was stirred in methanol (160 ml) and thionyl chloride (16.1 ml, 220.1 mmol, 1.4 eq) was added drop wise at r.t. and allowed to react for 18 hours. The reaction was then evaporated under vacuum and then chased 4x methanol, 3x methylene chloride, 3x toluene, and 2x hexanes to produce a quantitative yield of the dimethyl-L-aspartate ester hydrochloride salt **15**.

Cti072505p68\_2

<sup>1</sup>H-NMR (400 MHz, CDCl<sub>3</sub>) ppm 8.76 (s, 2H) ppm 4.61 (d, 1H, J=4.1Hz) ppm 3.84 (s, 3H) ppm 3.75 (s, 3H) ppm 3.35 (dd, 1H, J=4.0Hz, J=18.0Hz) ppm 3.25 (dd, 1H, J=5.0Hz, J=17.9Hz)

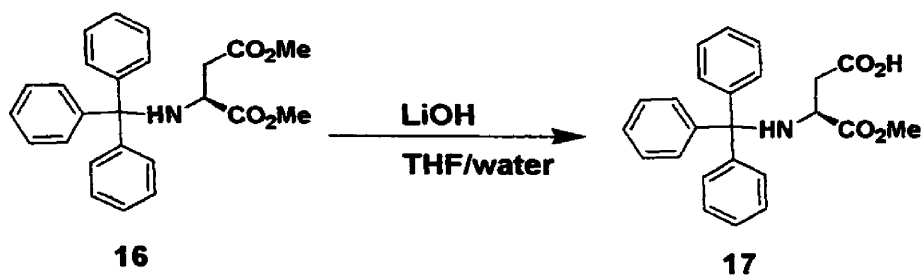


Dimethyl-L-aspartate ester hydrochloride salt **15** (38.0 g, 192.1 mmol) was stirred in methylene chloride (200 ml) with trityl chloride (48.3 g, 173.0 mmol, .9 eq).

Triethylamine (67.0 ml, 480 mmol, 2.5 eq) was added drop wise to the reaction at r.t. and was allowed to react for 18 hours. The reaction was then taken up in diethyl ether and rinsed through a silica plug. The ether was then evaporated under vacuum to produce a thick yellow oil of the N-trityl dimethyl L-aspartate **16** in near quantitative yield.

Cti072905p80\_1

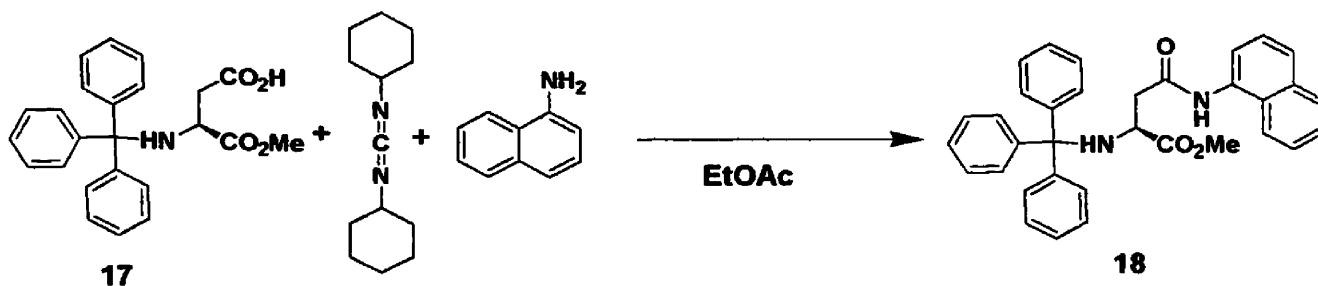
<sup>1</sup>H-NMR (400 MHz, CDCl<sub>3</sub>) ppm 7.50 (d, 6H, J=7.7Hz) ppm 7.27 (t, 6H, J=7.7Hz) ppm 7.19 (t, 3H, J=7.3Hz) ppm 3.68 (s, 3H) ppm 3.27 (s, 3H) ppm 2.66 (dd, 1H, J=5.3Hz, J=14.7Hz) ppm 2.52 (dd, 1H, J=6.8Hz, J=14.7Hz)



N-trityl dimethyl L-aspartate **16** (69.7 g, 173 mmol) was stirred in THF /water (200 ml, 10 ml) and LiOH monohydrate (9.45 g, 225 mmol, 1.3 eq) was added to the solution. The reaction was allowed to proceed at room temperature and monitored by TLC using a 10% MeOH/ methylene chloride mobile phase. After two hours the reaction was taken up in water with diethyl ether. The water layer was kept and EtOAc was added to create a biphasic system. A 2M ammonium chloride solution (20 ml) was added to protonate the acid. The water layer was extracted two more times with EtOAc and the fractions were combined and evaporated under vacuum to produce a fine flaky very light yellow solid of the monomethyl ester of N-trityl L-aspartate **17**.

Cti093005p108\_2

<sup>1</sup>H-NMR (400 MHz, CDCl<sub>3</sub>) ppm 7.46 (d, 1H, J=7.5Hz) ppm 7.19 (t, 6H, J=7.1Hz) ppm 7.13 (d, 3H, J=6.9Hz) ppm 3.57 (s, 1H) ppm 3.13 (s, 3H) ppm 2.49 (dd, 1H, J=7.2Hz, J=15.5Hz) ppm 2.29 (dd, 1H, J=6.1Hz, J=13.5Hz)

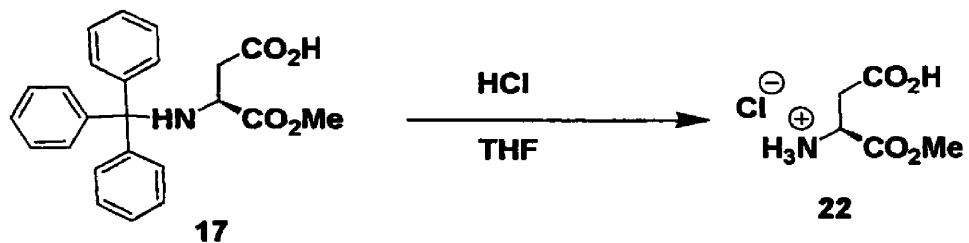


The monomethyl ester **17** (1.39 g, 3.57 mmol) and 2-naphthylamine (.510 g, 3.57 mmol, 1.0 eq) were dissolved in 20 ml of ice cold EtOAc. Dicyclohexylcarbodiimide (1.43 g, 6.94 mmol, 1.94 eq) was added in two instances. Once to the cold EtOAc reaction solution (.808 g, 3.93 mmol, 1.1 eq) and then once 14 hours later (.622 g, 3.01 mmol, .84 eq) right before the work up of the reaction (TLC with 10% MeOH/methylene chloride seemed to show that all of the starting material was gone). The reaction was filtered through about 50 ml of silica and then concentrated under vacuum. To the concentrate was added hexanes until a light purple precipitate formed. The precipitate was filtered away from the solution and shown by <sup>1</sup>H NMR to be the desired product **18** in a 30% yield.

Cti080105p84\_1

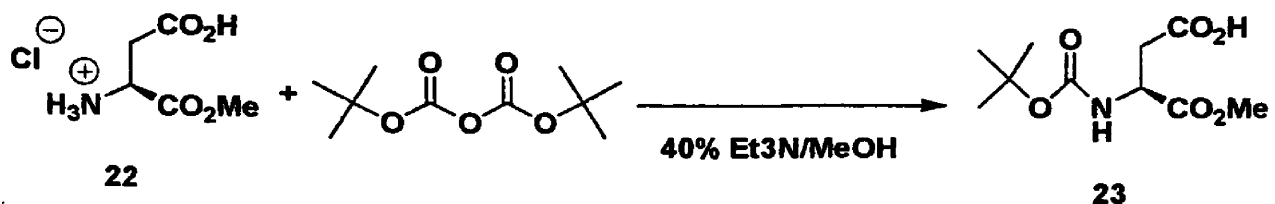
<sup>1</sup>H-NMR (400 MHz, CDCl<sub>3</sub>) ppm 8.81 (s, 1H) ppm 8.00 (d, 1H, J=7.5Hz) ppm 7.91 (d, 1H, J=8.4Hz) ppm 7.86 (d, 1H, J=8.1Hz) ppm 7.67 (d, 1H, J=8.2Hz) ppm 7.52 (d, 6H, J=7.7Hz) ppm 7.46 (dd, 2H, J=7.2Hz, J=14.7Hz) ppm 7.40 (m, 1H) ppm 7.27 (ddd, 9H, J=4.4Hz, J=10.5Hz, J=20.6Hz) ppm 3.87 (s, 1H) ppm 3.53 (s, 3H) ppm 2.64 (dd, 1H, J=4.0Hz, J=14.8Hz) ppm 2.06 (dd, 1H, J=5.5Hz, J=14.8Hz)





The monomethyl ester **17** (7.71 g, 19.82 mmol) was stirred in 20 ml THF. To the reaction was added 30 ml of a 2M solution of HCl (60.0 mmol, 3.03 eq). The reaction was monitored by TLC UV and ninhydrin with 10% MeOH/ methylene chloride as the mobile phase. After completion the reaction was taken up in water and ethyl ether and extracted. The water layer containing **22** was carried on to the next reaction crude.

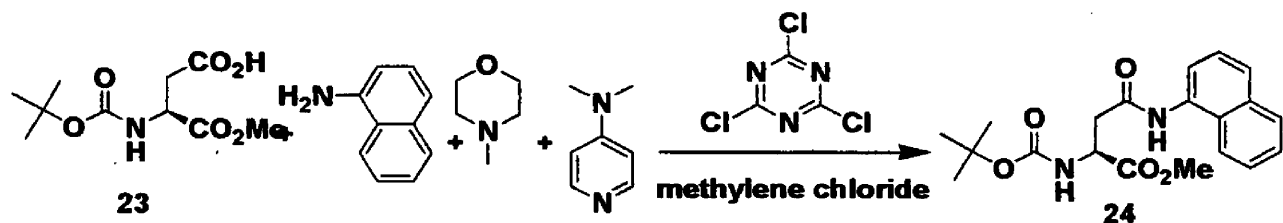
No NMR file



The triethylamine (28.0 ml, 20.31 mmol, 1.02 eq) and methanol (70 ml) were added to the water fraction from the previous reaction and then the Boc anhydride (7.41 g, 34.0 mmol, 1.7 eq) was added and the reaction was allowed to proceed overnight. The reaction was then evaporated under vacuum and again taken up in water and ether. The water layer was kept and stirred with ethyl acetate while the pH was adjusted to about 2 using litmus paper as an indicator. The water layer was extracted two more times with ethyl acetate. The organic layers were then combined and dried over magnesium sulfate and evaporated to dryness. The ethyl acetate was chased with methylene chloride to produce a yellow oil of **23** in a 65% yield using **17** as the starting material for the entire reaction.

Cti101805p135\_1

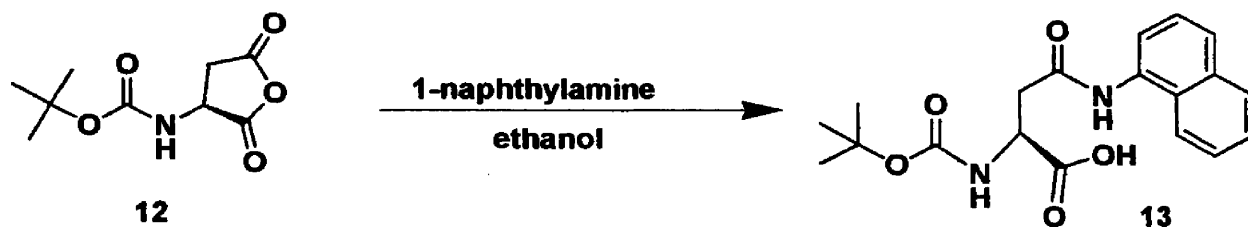
<sup>1</sup>H-NMR (400 MHz, CDCl<sub>3</sub>) ppm 7.25 (s, 1H) ppm 6.70 (m, 1H) ppm 6.44 (s, 1H) ppm 5.57 (dd, 1H, J=8.0Hz, J=19.7Hz) ppm 4.61 (s, 1H) ppm 3.76 (s, 3H) ppm 3.07 (d, 1H, J=20.5Hz) ppm 2.88 (d, 1H, J=17.1Hz) ppm 1.45 (m, 9H)



The Boc protected monomethyl ester **23** (.435 g, 1.76 mmol) was added to 40 ml of methylene chloride along with N-methylmorpholine (.29 ml, 2.64 mmol, 1.5 eq), 2-naphthylamine (.251 g, 1.76 mmol, 1.0 eq), and dimethylaminopyridine (DMAP, .02g, .176 mmol, 0.1eq) as a catalyst. Finally, cyanuric chloride (.097 g, .528 mmol, .3 eq) was added and the reaction was stirred at r.t. for an hour. The reaction was filtered through a silica plug with methylene chloride and a fraction was taken. Then the silica plug was washed with 10% MeOH/methylene chloride and this wash was kept and evaporated to dryness. The fraction was chased three times with methylene chloride to leave a purple solid of **24**.

cti101905p136\_1

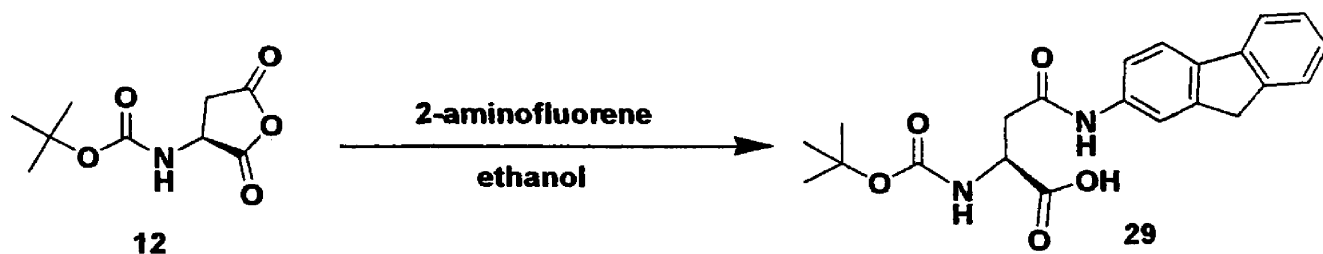
<sup>1</sup>H-NMR (400 MHz, CDCl<sub>3</sub>) ppm 7.82 (m, 2H) ppm 7.46 (m, 2H) ppm 7.31 (d, 1H, J=2.8Hz) ppm 7.29 (s, 1H) ppm 6.80 (d, 1H, J=6.5Hz) ppm 4.59 (dd, 1H, J=7.7Hz, J=10.6Hz) ppm 3.76 (s, 1H) ppm 1.45 (s, 9H)



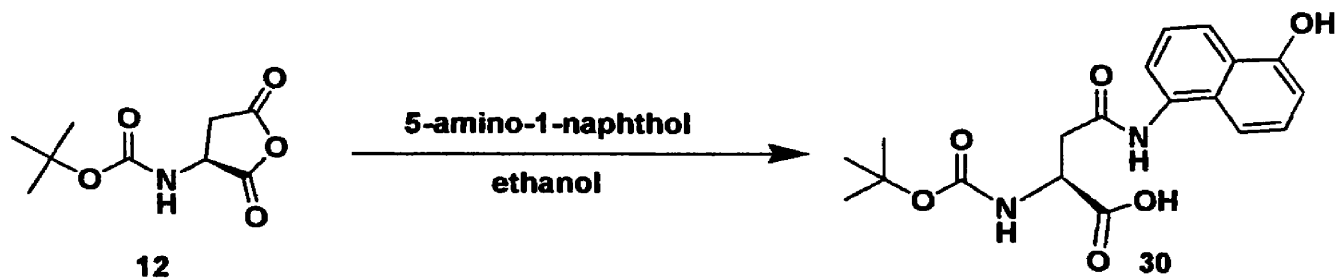
The L-aspartic anhydride **12** (3.00 g, 12.8 mmol) was stirred in 30-40 ml ethanol. 2-aminofluorene (1.84 g, 12.8 mmol, 1.0 eq) was added and the reaction was allowed to proceed 4 hours at r.t. The reaction was evaporated under vacuum to purple solid. The reaction mixture was chromatographed (10% MeOH/ CH<sub>2</sub>Cl<sub>2</sub>) to give .100 g of the pure **13**, a 2% yield.

Cti121405p176\_1

<sup>1</sup>H-NMR (400 MHz) ppm 9.94 (s, 1H) ppm 8.10 (m, 1H) ppm 7.93 (m, 1H) ppm 7.76 (d, 1H, J=8.1Hz) ppm 7.66 (d, 1H, J=7.4Hz) ppm 7.54 (dd, 1H, J=5.0Hz, J=9.0Hz) ppm 7.49 (dd, 1H, J=7.8Hz) ppm 7.17 (d, 1H, J=8.3Hz) ppm 4.43 (dd, 1H, J=7.8Hz, J=14.0Hz) ppm 2.94 (dd, 1H, J=5.6Hz, J=15.0Hz) ppm 2.83 (dd, 1H, J=8.0Hz, J=15.0Hz) ppm 1.39 (s, 9H)



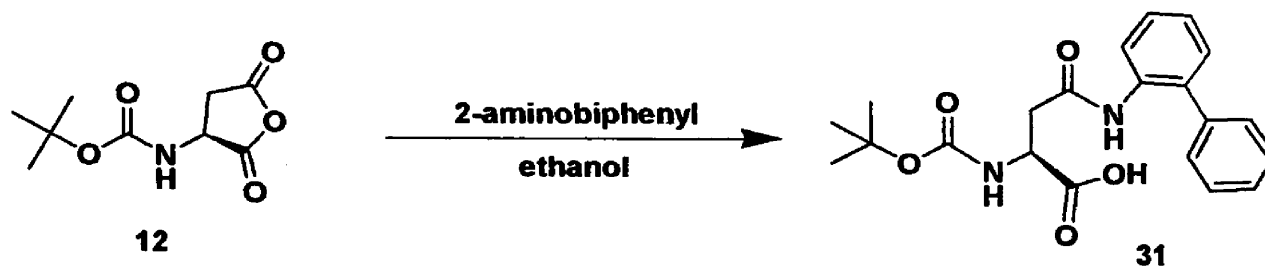
The L-aspartic anhydride **12** (3.00 g, 12.8 mmol) was stirred in 30-40 ml ethanol. 2-aminofluorene (2.32 g, 12.8 mmol, 1.0 eq) was added and the reaction was allowed to proceed 4 hours at r.t. The reaction was evaporated under vacuum to a yellow oil. The reaction mixture was chromatographed (10% MeOH/ CH<sub>2</sub>Cl<sub>2</sub>) to give .100 g of the pure **29**, a 2% yield.



The L-aspartic anhydride **12** (3.00 g, 12.8 mmol) was stirred in 30-40 ml ethanol. 5-amino-1-naphthol (2.05 g, 12.8 mmol, 1.0 eq) was added and the reaction was allowed to proceed 4 hours at r.t. The reaction was evaporated under vacuum to dark oil. The reaction mixture was chromatographed first with (50% EtOAc/hexanes) and then followed with (20% MeOH/ CH<sub>2</sub>Cl<sub>2</sub>) to elute .372 g of the pure **30**, an 8% yield.

Cti121605p164\_2

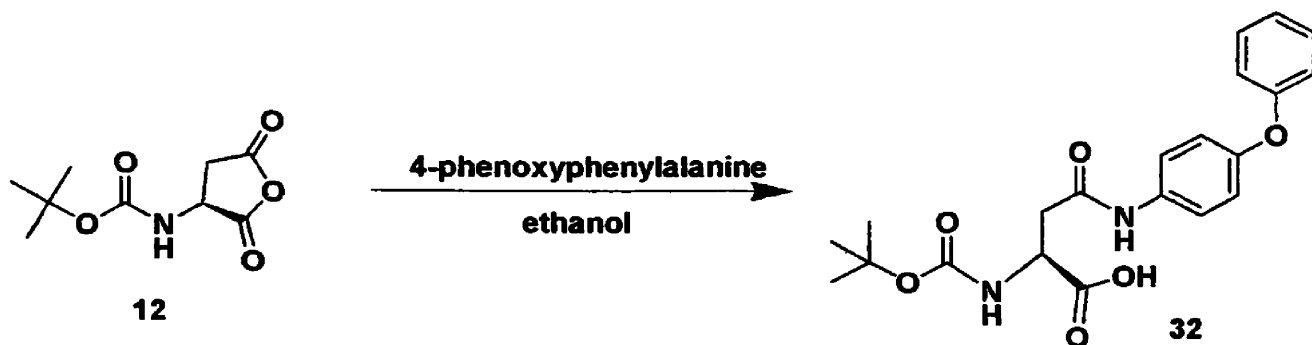
<sup>1</sup>H-NMR (400 MHz) ppm 9.54 (s, 1H) ppm 7.28 (dd, 1H, J=8.6Hz) ppm 7.14 (d, 1H, J=6.4Hz) ppm 6.99 (d, 1H, J=7.7Hz) ppm 6.71 (dd, 1H, J=7.4Hz) ppm 6.62 (dd, 1H, J=7.8Hz) ppm 6.22 (d, 1H, J=7.4Hz) ppm 5.84 (s, 1H) ppm 3.47 (m, 1H) ppm 2.20 (dd, 1H, J=5.2Hz, J=14.8Hz) ppm 2.01 (dd, 1H, J=4.5Hz, J=13.4Hz) ppm 0.71 (s, 1H)



The L-aspartic anhydride **12** (3.05 g, 14.2 mmol) was stirred in 30-40 ml ethanol. 2-aminobiphenyl (2.25 g, 13.3 mmol, .9 eq) was added and the reaction was allowed to proceed 4 hours at r.t. The reaction was evaporated under vacuum to a yellow oil. The reaction mixture was chromatographed first with (50% EtOAc/ hexanes) and then followed with (20% MeOH/ CH<sub>2</sub>Cl<sub>2</sub>) to elute .372 g of the pure **31**, a 7% yield.

Cti120505p172\_2

<sup>1</sup>H-NMR (400 MHz, CDCl<sub>3</sub>) ppm 8.08 (d, 1H, J=5.4Hz) ppm 7.37 (m, 1H) ppm 5.81 (s, 1H) ppm 5.55 (s, 1H) ppm 4.55 (m, 1H) ppm 4.14 (dd, 1H, J=6.6Hz, J=13.0Hz) ppm 3.00 (d, 1H, J=17.2Hz) ppm 2.82 (d, 1H, J=16.9Hz) ppm 1.43 (s, 9H)

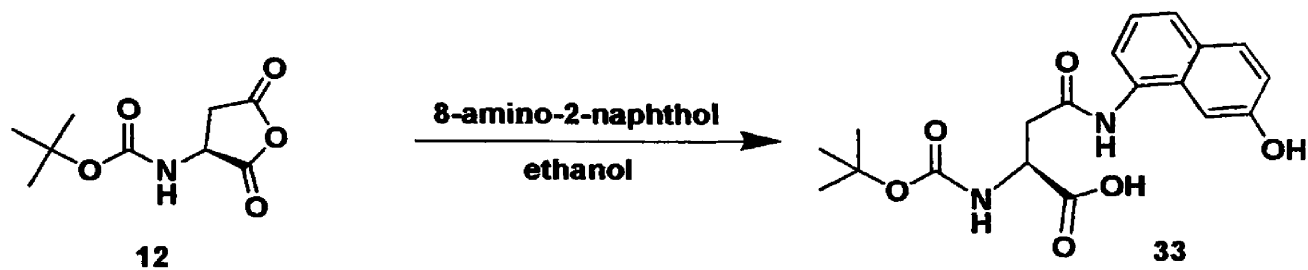


The L-aspartic anhydride **12** (3.00 g, 12.8 mmol) was stirred in 30-40 ml ethanol. 4-phenoxyphenylalanine (2.38 g, 12.8 mmol, 1.0 eq) was added and the reaction was allowed to proceed 4 hours at r.t. The reaction was evaporated under vacuum to a dark oil. The alpha addition product crystallized as a white solid (.727 g, 1.8 mmol) from the reaction mixture over two days. The remaining reaction mixture was chromatographed (10% MeOH/ CH<sub>2</sub>Cl<sub>2</sub>) to give .352 g of the pure **32**, a 3% yield.

Cti121405p166\_3

<sup>1</sup>H-NMR (400 MHz, CDCl<sub>3</sub>) ppm 7.45 (d, 2H, J=6.1Hz) ppm 7.32 (m, 2H) ppm 7.09 (m, 1H) ppm 6.97 (m, 4H) ppm 5.96 (s, 1H) ppm 4.53 (m, 1H) ppm 3.11 (m, 1H) ppm 2.92 (m, 1H) ppm 1.44 (s, 9H)

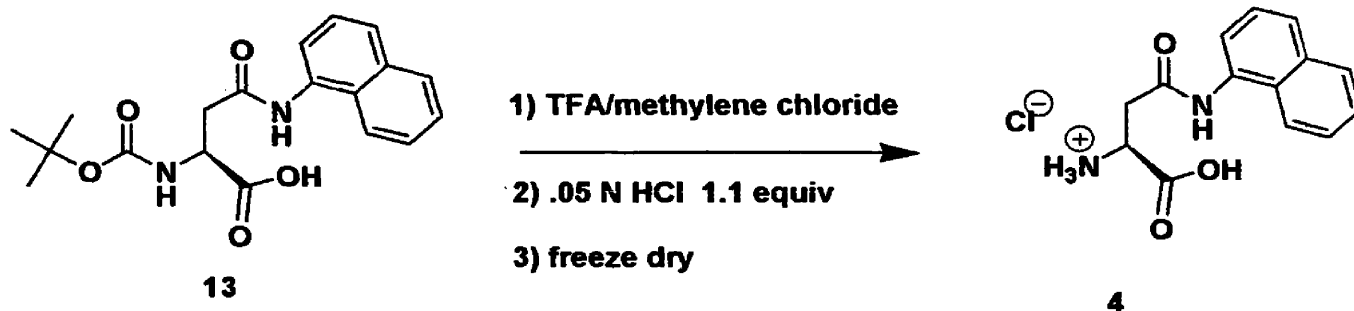




The L-aspartic anhydride **12** (3.00 g, 12.8 mmol) was stirred in 30-40 ml ethanol. 8-amino-2-naphthol (2.05 g, 12.8 mmol, 1.0 eq) was added and the reaction was allowed to proceed 4 hours at r.t. The reaction was evaporated under vacuum to a dark oil. The reaction mixture was chromatographed (10% MeOH/ CH<sub>2</sub>Cl<sub>2</sub>) to give .336 g of the pure **33**, a 7% yield.

Cti121405p162\_1

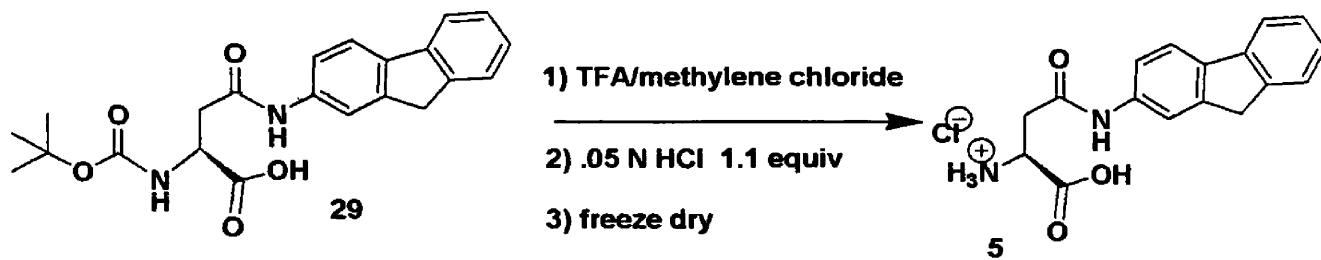
<sup>1</sup>H-NMR (400 MHz, d<sub>6</sub>-DMSO) ppm 7.74 (d, 1H, J=8.8Hz) ppm 7.69 (d, 1H, J=6.4Hz) ppm 7.56 (d, 1H, J=8.0Hz) ppm 7.44 (s, 1H) ppm 7.20 (dd, 1H, J=7.8Hz) ppm 7.09 (dd, 1H, J=1.8Hz, J=8.8Hz) ppm 6.46 (s, 1H) ppm 4.11 (m, 1H) ppm 2.82 (dd, 1H, J=7.0Hz, J=14.5Hz) ppm 2.64 (dd, 1H, J=4.3Hz, J=15.5Hz) ppm 1.38 (s, 9H)



The Boc protected N-naphthyl aspartic acid **13** (.093 g, .260 mmol) was stirred in TFA (1.5 ml, 8.87 mmol, 34 eq) and methylene chloride (4ml). The reaction was monitored using TLC, UV and ninhydrin, and 10% MeOH/methylene chloride as the mobile phase. The reaction was stopped upon the disappearance of **13** at close to 30 minutes from the start of the reaction. The solution was evaporated to dryness at r.t. and then stirred in ethyl ether. The solid was filtered away and then taken up in a .05 N solution of HCl (9 ml, .450 mmol, 1.7 eq) and stirred until the solid had broken up. The solution was then frozen and the water evaporated under reduced pressure to leave .05 g of a purple powder of **4**, a 65% yield.

Cti110305p153\_1

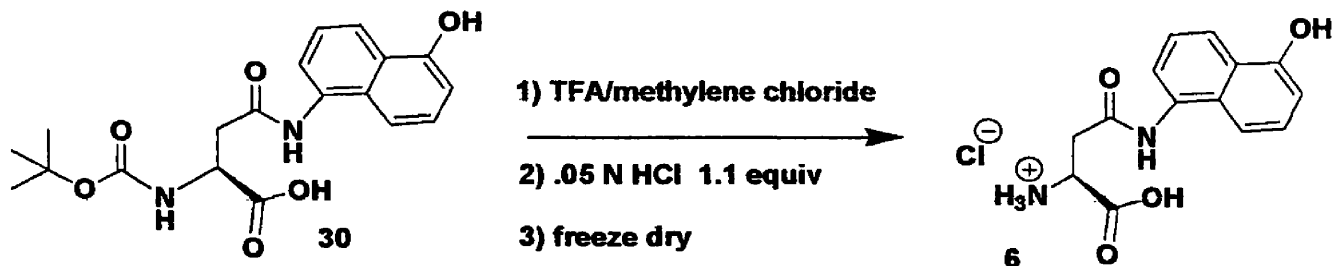
<sup>1</sup>H-NMR (400 MHz, D<sub>2</sub>O) ppm 7.76 (d, 1H, J=9.2Hz) ppm 7.70 (d, 1H, J=7.7Hz) ppm 7.37 (m, 1H) ppm 7.33 (t, 1H, J=7.8Hz) ppm 4.26 (t, 1H, J=5.4Hz) ppm 3.17 (dd, 1H, J=5.8Hz, J=16.9Hz) ppm 3.11 (dd, 1H, J=5.1Hz, J=17.0Hz)



The Boc protected N-fluorenyl aspartic acid **29** (.05 g, .126 mmol) was stirred in TFA (1.5 ml, 8.87 mmol, 70 eq) and methylene chloride (4ml). The reaction was monitored using TLC, UV and ninhydrin, and 10% MeOH/methylene chloride as the mobile phase. The reaction was stopped upon the disappearance of **29** at close to 50 minutes from the start of the reaction. The solution was evaporated to dryness at r.t. and then stirred in ethyl ether. The solid was filtered away and then taken up in a .05 N solution of HCl (2.7 ml, .139 mmol, 1.1 eq) and stirred until the solid had broken up. The solution was then frozen and the water evaporated under reduced pressure to leave .027 g of a purple powder of **5**, a 64% yield.

Ct111705p32\_1

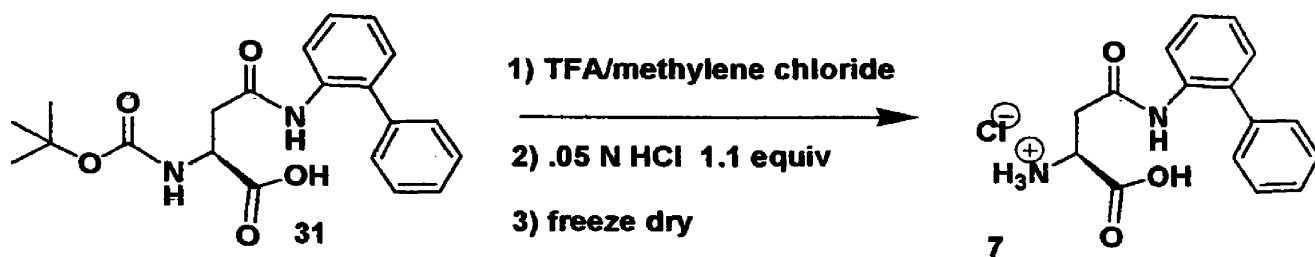
<sup>1</sup>H-NMR (400 MHz, d<sub>6</sub>-DMSO) ppm 10.65 (s, 1H) ppm 7.93 (s, 1H) ppm 7.82 (d, 1H, J=2.6Hz) ppm 7.80 (d, 1H, J=4.9Hz) ppm 7.56 (d, 1H, J=5.9Hz) ppm 7.53 (d, 1H, J=8.0Hz) ppm 7.35 (t, 1H, J=7.5Hz) ppm 7.26 (t, 1H, J=7.4Hz) ppm 3.90 (s, 2H) ppm 3.81 (dd, 1H, J=5.3Hz, J=6.6Hz) ppm 3.03 (dd, 1H, J=4.3Hz, J=16.7Hz) ppm 2.74 (dd, 1H, J=7.2Hz, J=15.5Hz)



The Boc protected N-5-hydroxynaphthyl-1-yl aspartic acid **30** (.05 g, .134 mmol) was stirred in TFA (1.5 ml, 8.87 mmol, 66 eq) and methylene chloride (4ml). The reaction was monitored using TLC, UV and ninhydrin, and 10% MeOH/methylene chloride as the mobile phase. The reaction was stopped upon the disappearance of **30** at close to 60 minutes from the start of the reaction. The solution was evaporated to dryness under vacuum at r.t. and then stirred in ethyl ether. The solid was filtered away and then taken up in a .05 N solution of HCl (3.0 ml, .147 mmol, 1.1 eq) and stirred until the solid had broken up. The solution was then frozen and the water evaporated under reduced pressure to leave .010 g of a purple powder of **6**, a 24% yield.

Cti11705p30\_1

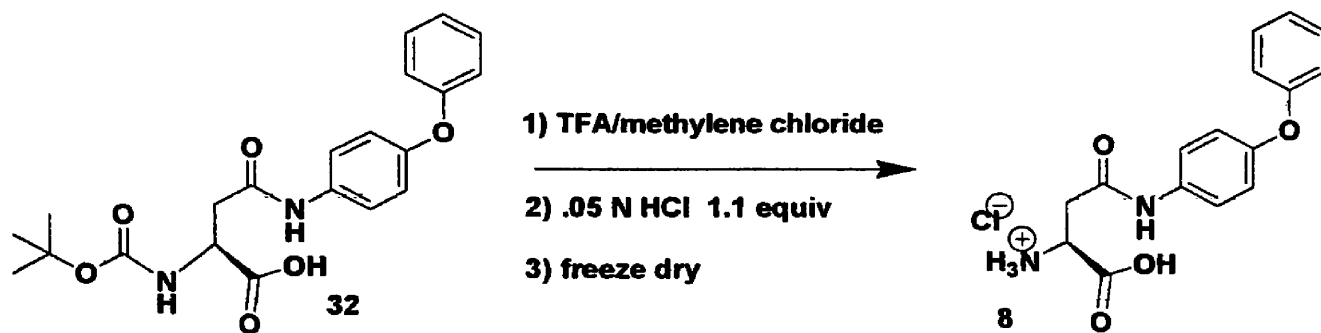
<sup>1</sup>H-NMR (400 MHz, d<sub>6</sub>-DMSO) ppm 8.00 (d, 1H, J=8.5Hz) ppm 7.65 (d, 1H, J=7.3Hz) ppm 7.53 (d, 1H, J=8.4Hz) ppm 7.41 (t, 1H, J=7.9Hz) ppm 7.33 (t, 1H, J=8.1Hz) ppm 6.91 (d, 1H, J=7.5Hz) ppm 4.29 (s, 1H) ppm 3.19 (dd, 1H, J=5.1Hz, J=17.0Hz) ppm 3.11 (dd, 1H, J=5.1Hz, J=17.0Hz)



The Boc protected N-biphen-2-yl aspartic acid **31** (.114g, .297 mmol) was stirred in TFA (1.5 ml, 8.87 mmol, 30 eq) and methylene chloride (4ml). The reaction was monitored using TLC, UV and ninhydrin, and 10% MeOH/methylene chloride as the mobile phase. The reaction was stopped upon the disappearance of **31** at close to 50 minutes from the start of the reaction. The solution was evaporated to dryness at r.t. and then stirred in ethyl ether. The solid was filtered away and then taken up in a .05 N solution of HCl (6.5 ml, .327 mmol, 1.1 eq) and stirred until the solid had broken up and dissolved. The solution was then frozen and the water evaporated under reduced pressure to leave .056 g of a purple powder of **7**, a 59% yield.

Cti120205p172\_1

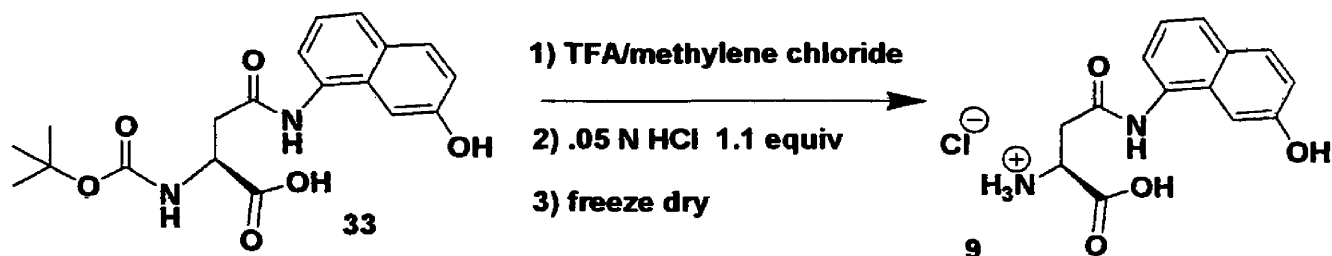
<sup>1</sup>H-NMR (400 MHz, d<sub>6</sub>-DMSO) ppm 9.61 (s, 1H) ppm 8.35 (s, 1H) ppm 7.36 (m, 9H) ppm 4.17 (dd, 1H, J=5.0Hz, J=9.4Hz) ppm 2.86 (dd, 1H, J=5.2Hz, J=17.2Hz) ppm 2.79 (dd, 1H, J=5.4Hz, J=17.0Hz)



The Boc protected N-4-phenoxyphenyl aspartic acid **32** (.10 g, .25 mmol) was stirred in TFA (1.5 ml, 8.87 mmol, 35 eq) and methylene chloride (4ml). The reaction was monitored using TLC, UV and ninhydrin, and 10% MeOH/methylene chloride as the mobile phase. The reaction was stopped upon the disappearance of **32** at close to 20 minutes from the start of the reaction. The solution was evaporated to dryness at r.t. and then stirred in ethyl ether. The solid was filtered away and then taken up in a .05 N solution of HCl (5.5 ml, .275 mmol, 1.1 eq) and stirred until the solid had broken up. The solution was then frozen and the water evaporated under reduced pressure to leave .047 g of a purple powder of **8**, a 56% yield.

Cti11705p166\_1

<sup>1</sup>H-NMR (400 MHz, d<sub>6</sub>-DMSO) ppm 10.48 (s, 1H) ppm 7.61 (d, 2H, J=8.6Hz) ppm 7.36 (t, 2H, J=7.6Hz) ppm 7.10 (t, 1H, J=7.3Hz) ppm 6.99 (d, 2H, J=8.5Hz) ppm 6.95 (d, 2H, J=8.3Hz) ppm 4.18 (dd, 1H, J=4.9Hz) ppm 3.03 (dd, 1H, J=4.8Hz, J=16.8Hz) ppm 2.94 (dd, 1H, J=5.8Hz, J=17.0Hz)



The Boc protected N-8-hydroxynaphthalene-2-yl aspartic acid **33** (.05 g, .134 mmol) was stirred in TFA (1.5 ml, 8.87 mmol, 66 eq) and methylene chloride (4ml). The reaction was monitored using TLC, UV and ninhydrin, and 10% MeOH/methylene chloride as the mobile phase. The reaction was stopped upon the disappearance of **33** at close to 60 minutes from the start of the reaction. The solution was evaporated to dryness under vacuum at r.t. and then stirred in ethyl ether. The solid was filtered away and then taken up in a .05 N solution of HCl (3.0 ml, .147 mmol, 1.1 eq) and stirred until the solid had broken up. The solution was then frozen and the water evaporated under reduced pressure to leave .023 g of a purple powder of **9**, a 55% yield.

Cti112105p28\_1

<sup>1</sup>H-NMR (400 MHz, d<sub>6</sub>-DMSO) ppm 10.13 (s, 1H) ppm 9.88 (s, 1H) ppm 7.79 (d, 1H, J=8.8Hz) ppm 7.65 (d, 1H, J=8.2Hz) ppm 7.54 (d, 1H, J=7.4Hz) ppm 7.31 (d, 1H, J=1.9Hz) ppm 7.24 (t, 1H, J=7.8Hz) ppm 7.15 (dd, 1H, J=2.2Hz, J=8.9Hz) ppm 4.30 (dd, 1H, J=4.4Hz, J=9.1Hz) ppm 3.19 (dd, 1H, J=5.1Hz, J=17.0Hz) ppm 3.12 (dd, 1H, J=5.8Hz, J=16.9Hz)

## References:

- Albini, N.; Auricchio, S.; Minisci, F.; (1985) Base Catalysis and Solvent Effect in the Synthesis of Aspartame. *Chem. Ind.*, 484-485.
- Albrecht J.; (1989) L-Glutamine stimulates the efflux of newly taken up glutamine from astroglia but not from synaptosomes of the rat. *Neuropharmacology*, **28**, 885-887.
- Bacci, A.; Sancini, G.; Verderio, C.; Armano, S.; Pravettoni, E.; Fesce, R.; Franceschetti, S.; Matteoli, M.; (2002) Block of glutamate-glutamine cycle between astrocytes and neurons inhibits epileptiform activity in the hippocampus. *J. Neurophysiol.*, **88**, 2302-2310.
- Barnett, N. L.; Pow, D. V.; Robinson, S. R.; (2000) Inhibition of Muller cell glutamine synthetase rapidly impairs the retinal response to light. *Glia*, **30**, 64-73.
- Broer, A.; Deitmer, J. W.; Broer, S.; (2004) Astroglial glutamine transport by system N is upregulated by glutamate. *Glia*, **48**, 298-310.
- Broer, A.; Albers, A.; Setiawan, I.; Edwards, R.; Chaudhry, F.; Lang, F.; Wagner, C.; Broer, S.; (2002) Regulation of the glutamine transporter SN1 by extracellular pH and intracellular sodium ions. *Journal of Physiology*, **539**, 1, 3-14.
- Broer, S.; Brookes, N.; (2001) Transfer of glutamine between astrocytes and neurons. *Journal of Neurochemistry*, **77**, 705-719.
- Chaudhry, F. A.; Reimer, R. J.; Krizaj, D.; Barber, D.; Storm-Mathisen, J.; Copenhagen, D. R.; Edwards, R. H.; (1999) Molecular analysis of system N suggests novel physiological roles in nitrogen metabolism and synaptic transmission. *Cell*, **99**, 769-780.



- Chaudhry, F.; Krizaj, D.; Larsson, P.; Reimer, R.; Wreden, C.; Storm-Mathisen, J.; Copenhagen, D.; Kavanaugh, M.; Edwards, R.; (2001) Coupled and uncoupled proton movement by amino acid transporter system N. *The EMBO Journal*, **20**, 24, 7041-7051.
- Dietmer, J.; Broer, A.; Broer, S.; (2003) Glutamine efflux from astrocytes is mediated by multiple pathways. *Journal of Neurochemistry*, **87**, 127-135.
- Fei, Y. J.; Sugawara, M.; Nakanishi, T.; Huang, W.; Wang, H.; Prasad, P. D.; Leibach, F. H.; Ganapathy, V.; (2000) Primary structure, genomic organization and functional and electrogenic characteristics of human system N1, a Na<sup>+</sup>- and H<sup>+</sup>-coupled glutamine transporter. *J. Biol. Chem.*, **275**, 23707-23717.
- Giacomelli, G.; Porcheddu, A.; Salaris, M.; (2003) Simple One-Flask Method for the Preparation of Hydroxamic Acids. *Organic Letters*, **5**, 15, 2715-2717.
- Greenfield, A.; Grosanu, C.; Dunlop, J.; McIlvain, B.; Carrick, T.; Jow, B.; Lu, Q.; Kowal, D.; Williams, J.; Butera, J.; (2005) Synthesis and biological activities of aryl-ether-, biaryl-, and fluorine-aspartic acid and diaminopropionic acid analogs as potent inhibitors of the high-affinity glutamate transporter EAAT-2. *Bioorganic and Medicinal Chemistry Letters*, **15**, 4985-4988.
- Kilberg, M. S.; Handlogten, M. E.; (1980) Christensen, H. N.; Characteristics of an amino acid transport system in rat liver for glutamine, asparagine, histidine and closely related analogues. *J. Biol. Chem.*, **255**, 4011-4019.
- Klausner, Y.; Bodansky, M.; (1972) Coupling Reagents in Peptide Synthesis. *Synthesis*, 453-463.

- Levenson, J.; Weeber, E.; Selcher, J. C.; Kategaya, L. S.; Sweatt, J. D.; Eskin, A.; (2002) Long-term potentiation and contextual fear conditioning increase neuronal glutamate uptake. *Nat. Neurosci.*, **5**, 155-161.
- Mackenzie, B.; Erickson, J.; (2004) Sodium-coupled neutral amino acid (System N/A) transporters of the SLC38 gene family. *Eur. J. Physiol.*, **447**, 784-795.
- McGale, E. H.; Pye, I. F.; Stonier, C.; Hutchinson, E. C.; Aber, G. M.; (1977) Studies of the inter-relationship between cerebrospinal fluid and plasma amino acid concentrations in normal individuals. *J. Neurochem.*, **29**, 291-297.
- Nagaraja, T. N.; Brookes, N.; (1996) Glutamine transport in mouse cerebral astrocytes. *J. Neurochem.*, **66**, 1665-1674.
- Rae, C.; Hare, N.; Bubb, W. A.; McEwan, S. R.; Broer, A.; McQuillan, J. A.; Balcar, V. J.; Conigrave, A. D.; Broer, S.; (2003) Inhibition of glutamine transport depletes glutamate and GABA neurotransmitter pools: further evidence for metabolic compartmentation. *J. Neurochem.*, **85**, 503-514.
- Ripley, J.; Watson, P.; Gajewski, M.; Warren, B.; Cybulski, K. A.; O'Brien, E.; Esslinger, S.; (2005) Synthetic glutamine analogues as inhibitors of the neutral amino acid transporter. Society for Neuroscience Poster Presentation Washington, D.C.
- Yang, C.; Su, C.; (1986) Effects of Solvents and additives on the reaction of N-benzyloxycarbonyl-L-aspartic anhydride with L-phenylalanine methyl ester (synthesis of aspartame). *J. Org. Chem.*, **51**, 5186-5191.

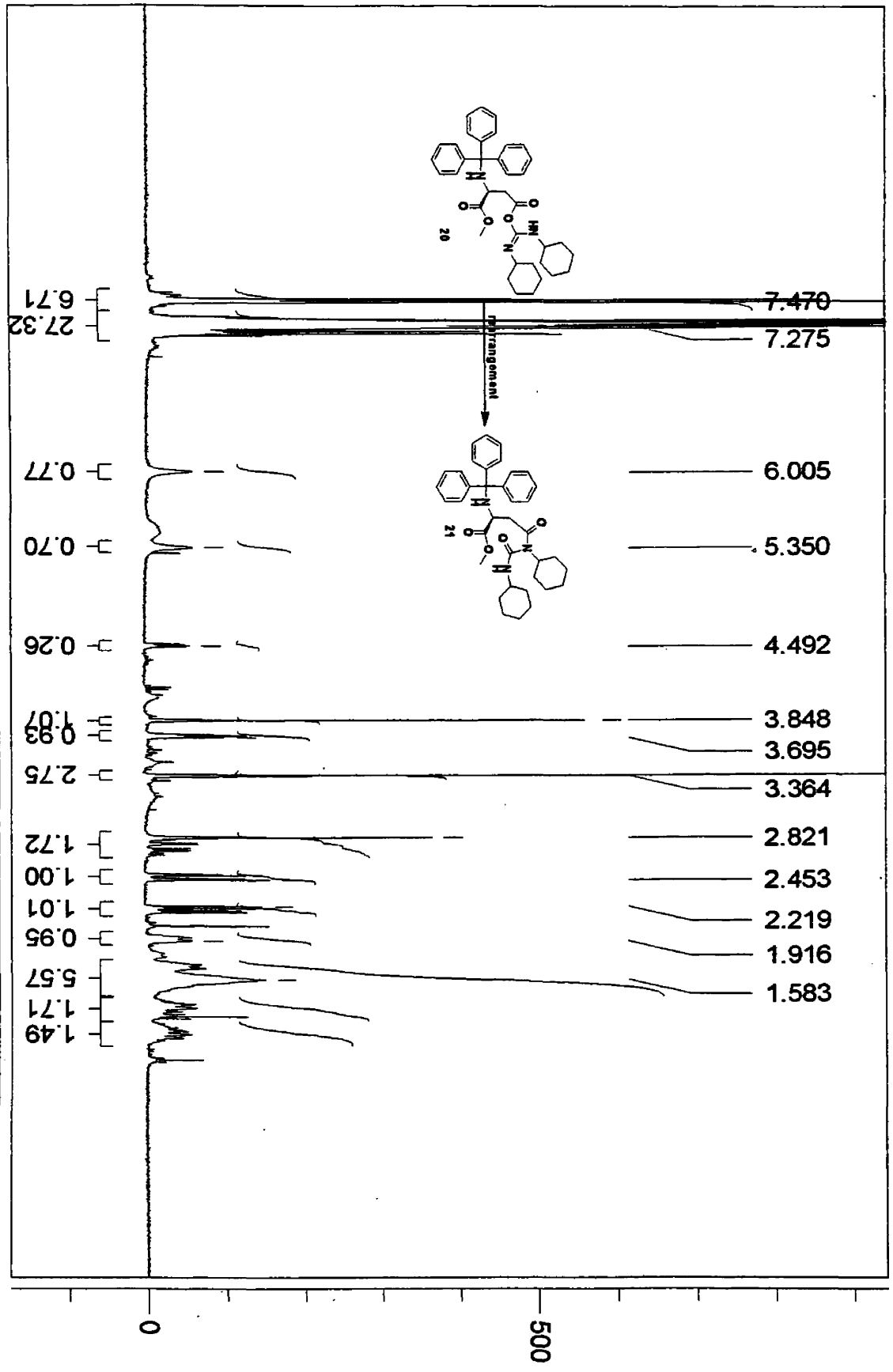
## **Appendices**

ppm (t1)

cti080905p98\_1 (Trasp naphthyl in d-CCl3)

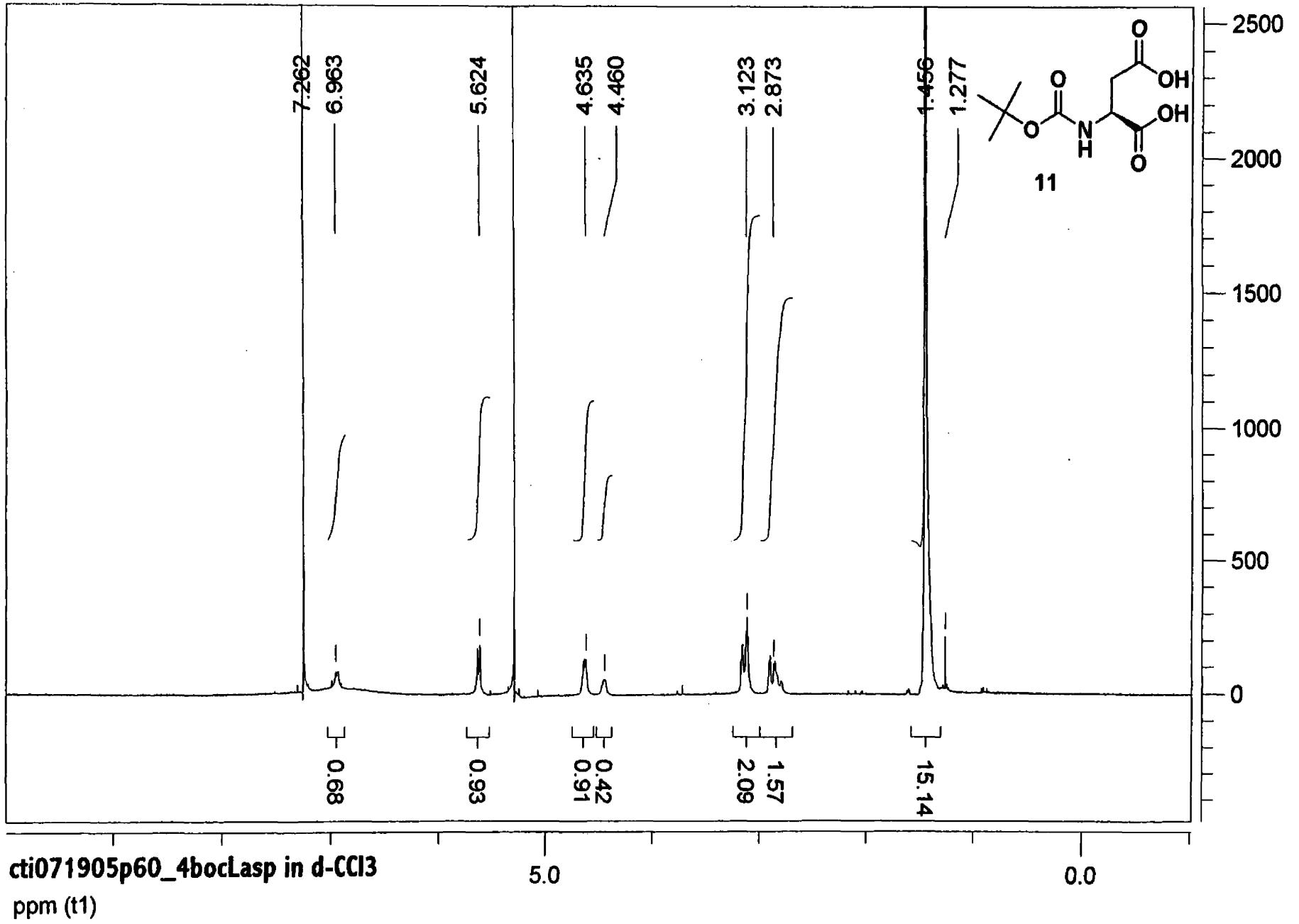
5.0

0.0



500

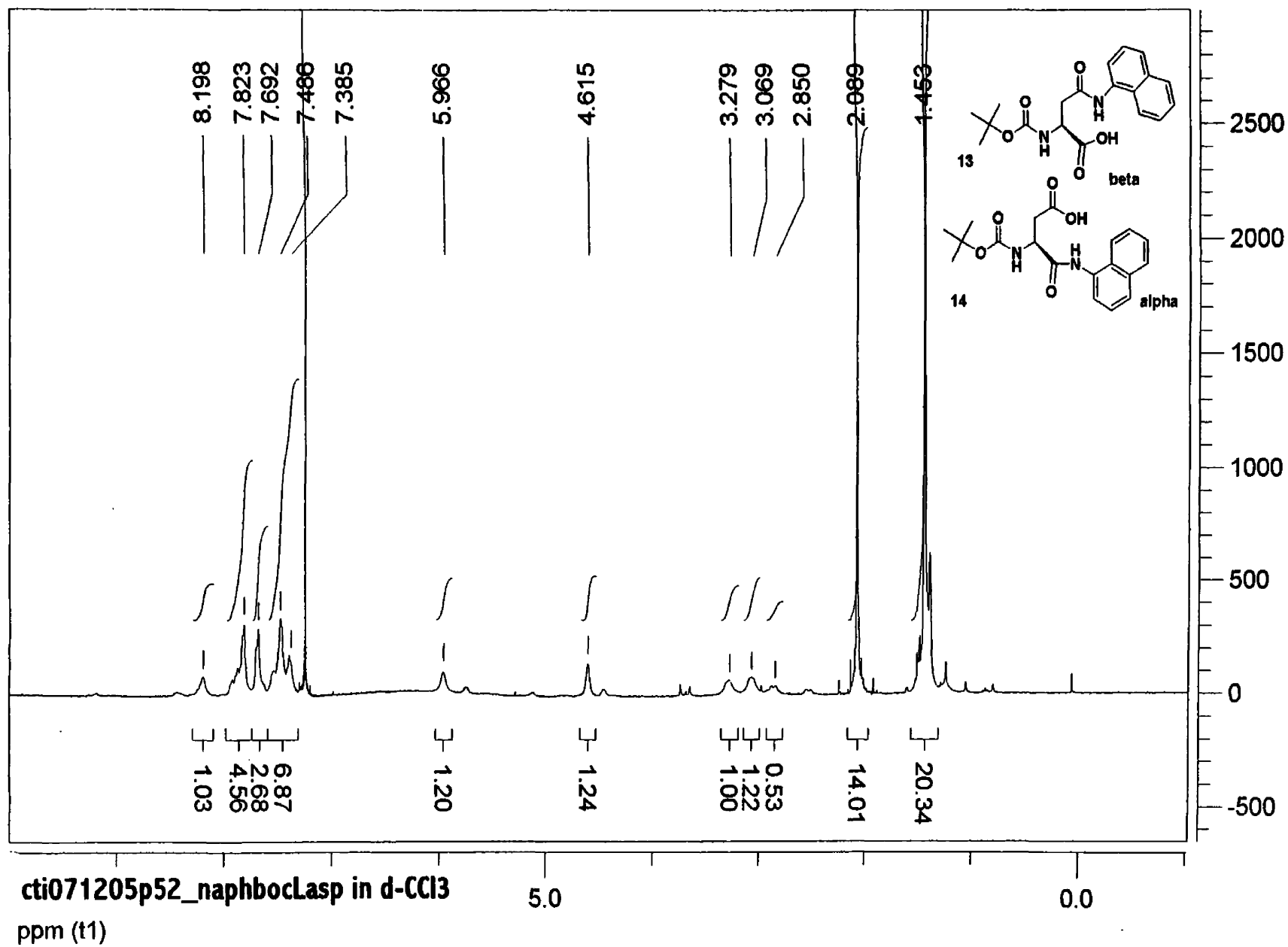
0

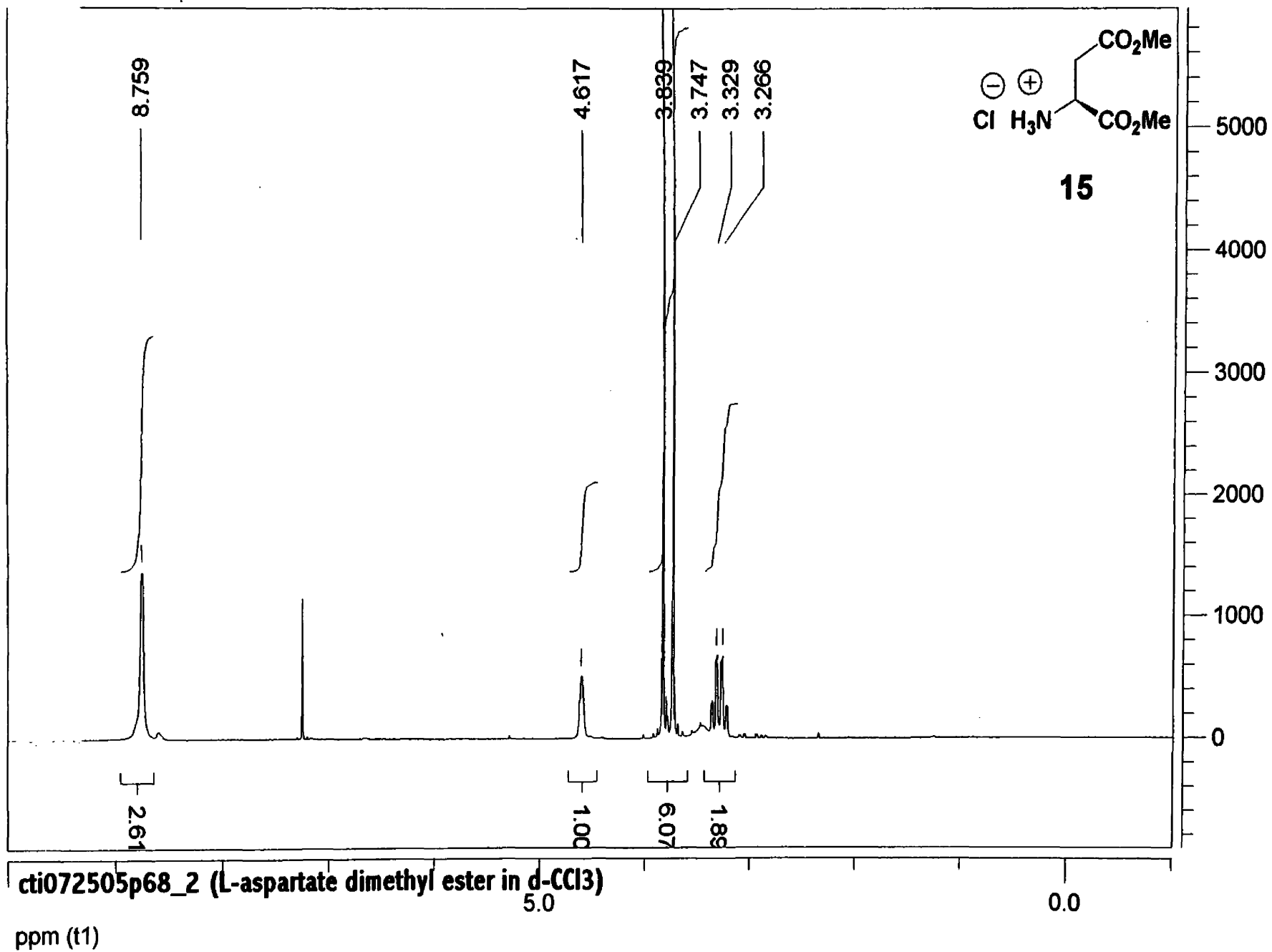


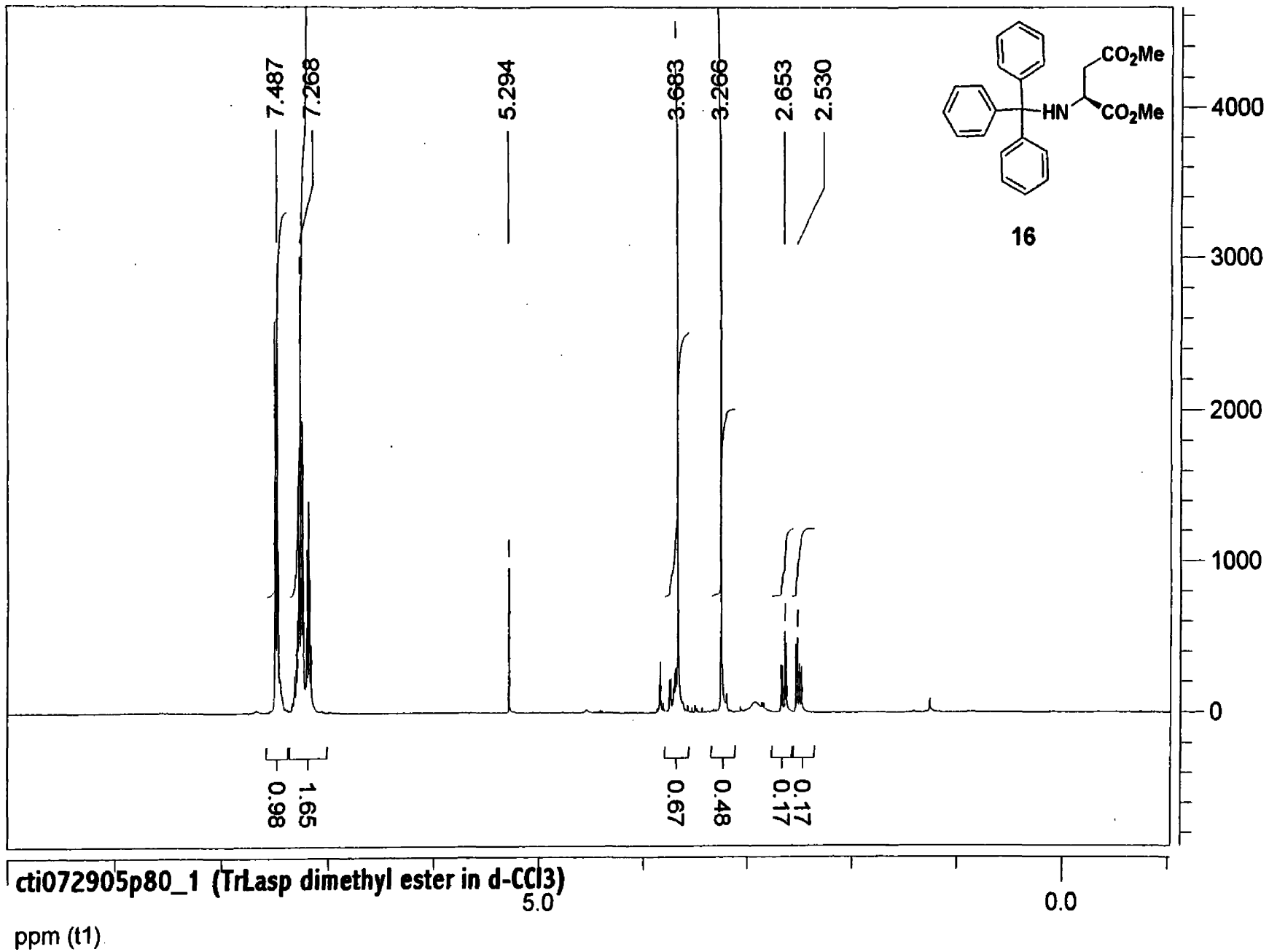
cti071905p60\_4bocLasp in d-CCl3  
ppm (t1)

5.0

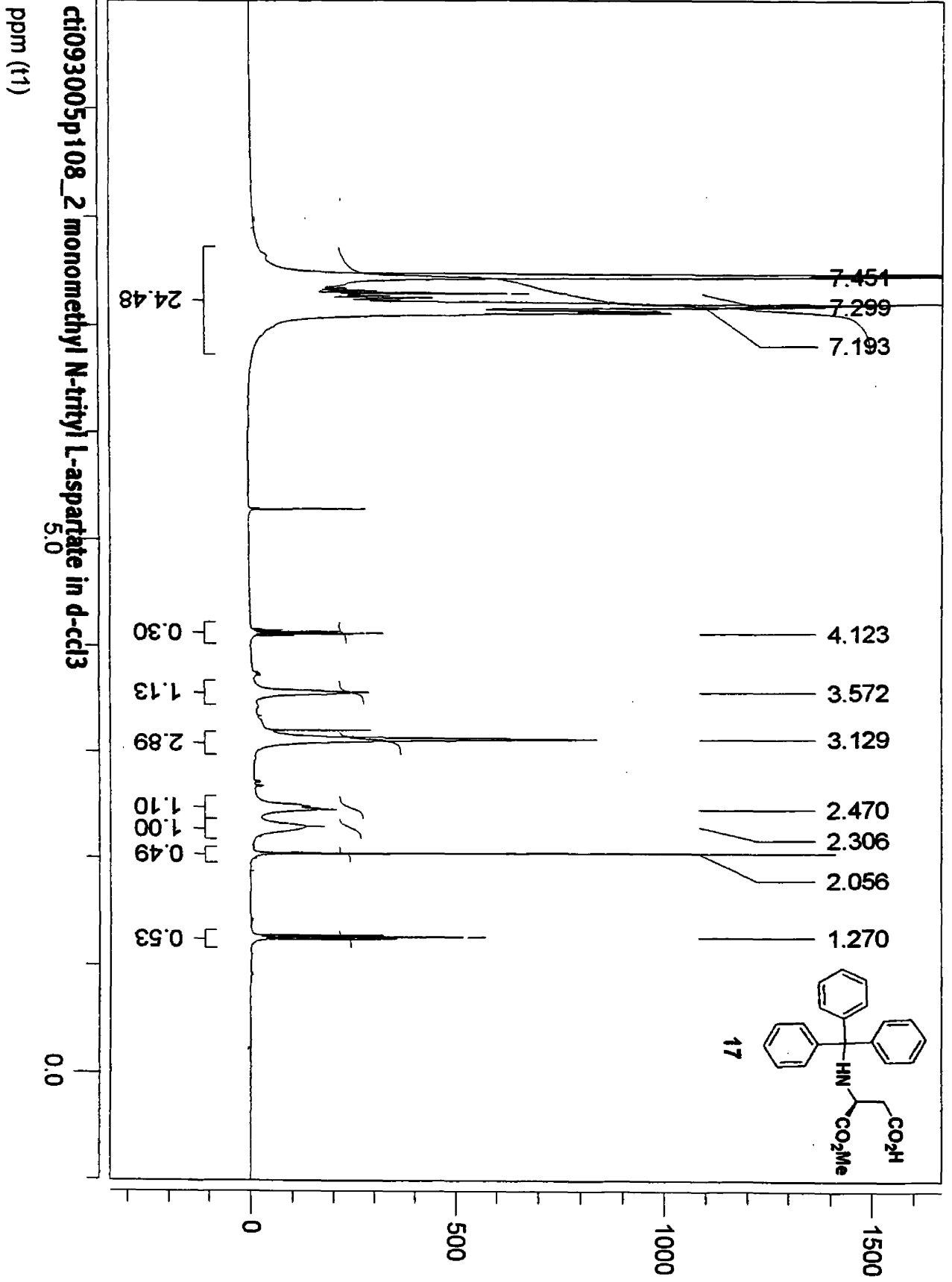
0.0

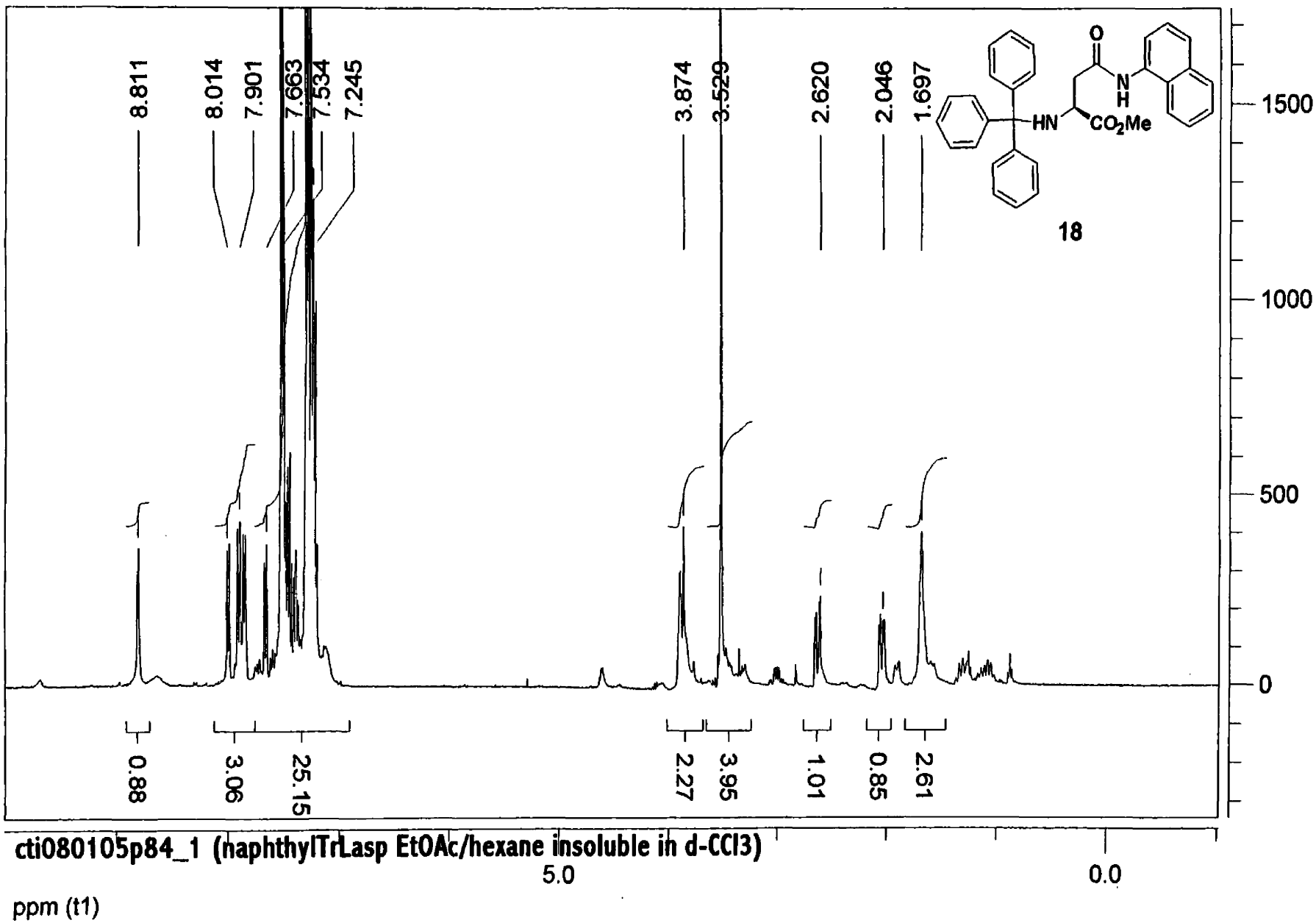






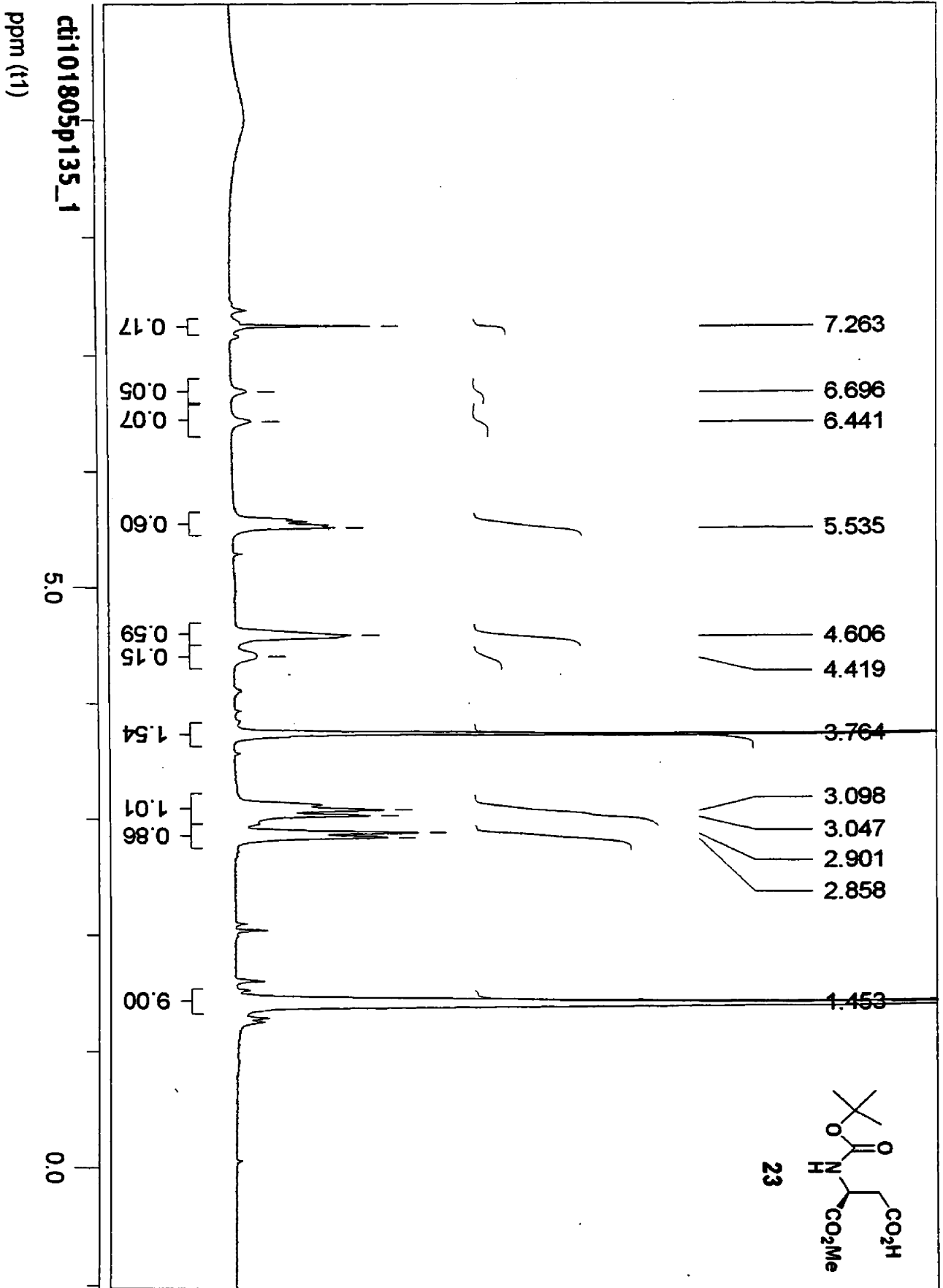




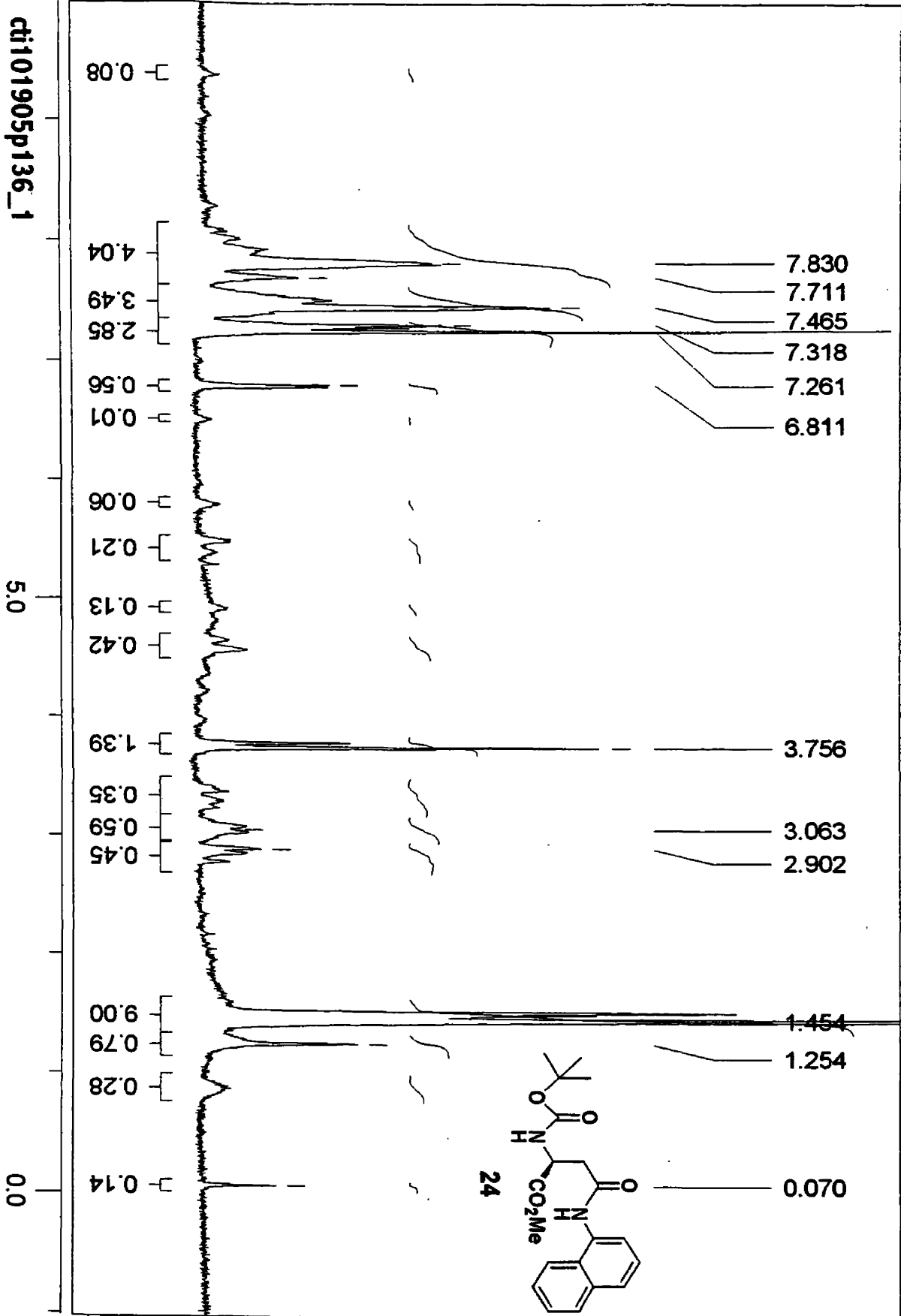


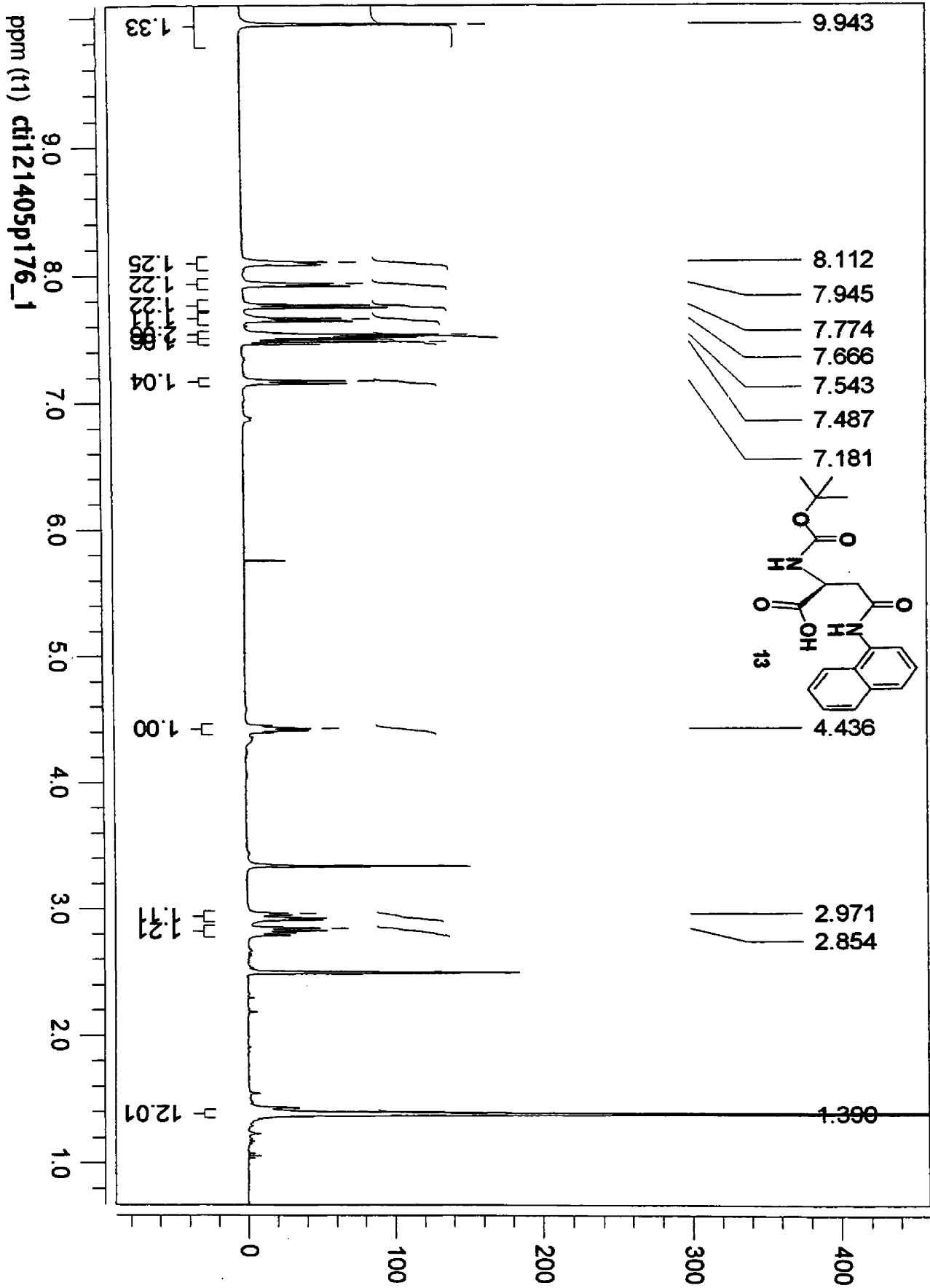
cti080105p84\_1 (naphthylTrLasp EtOAc/hexane insoluble in d-CCl3)

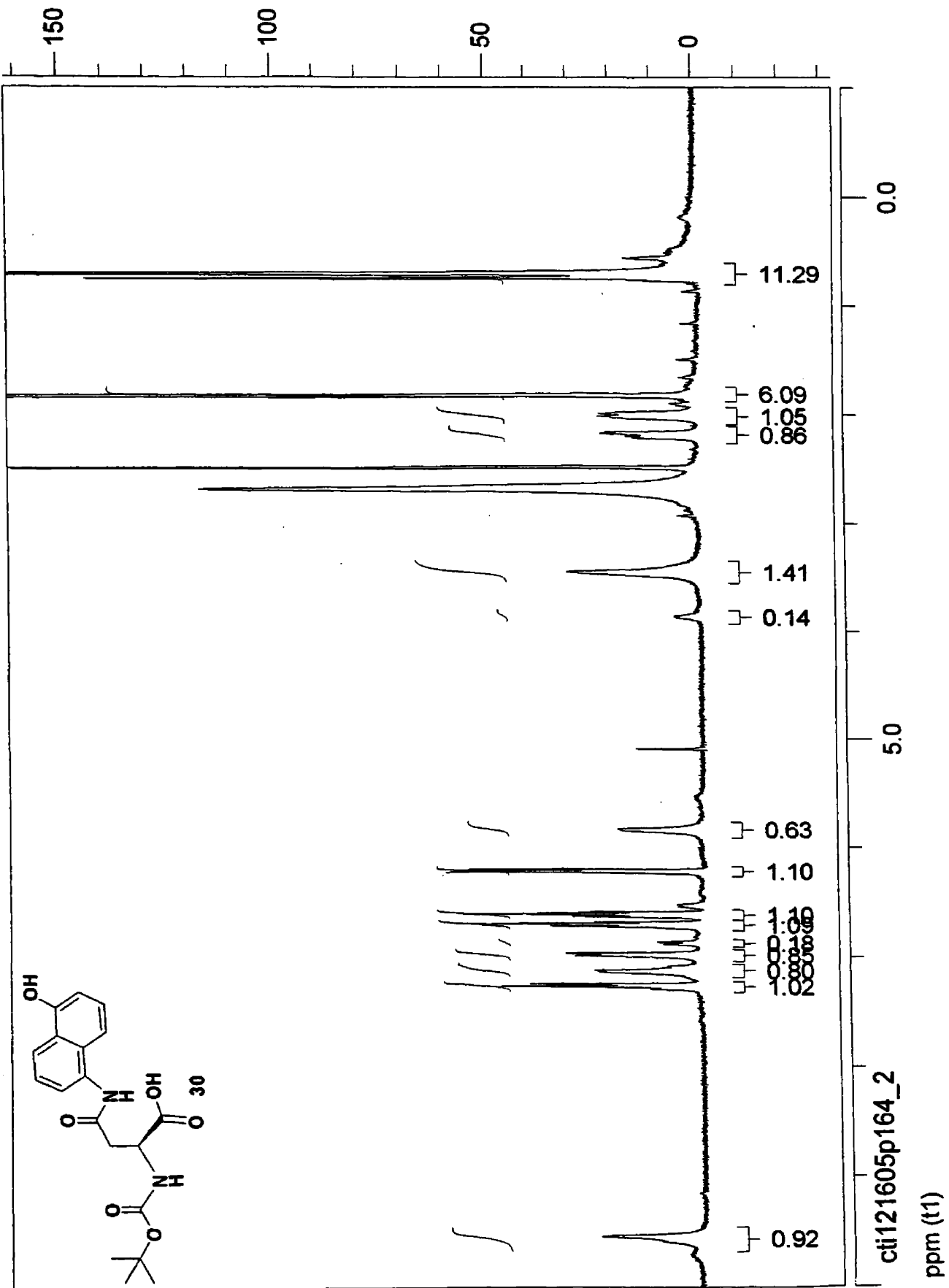
ppm (t1)

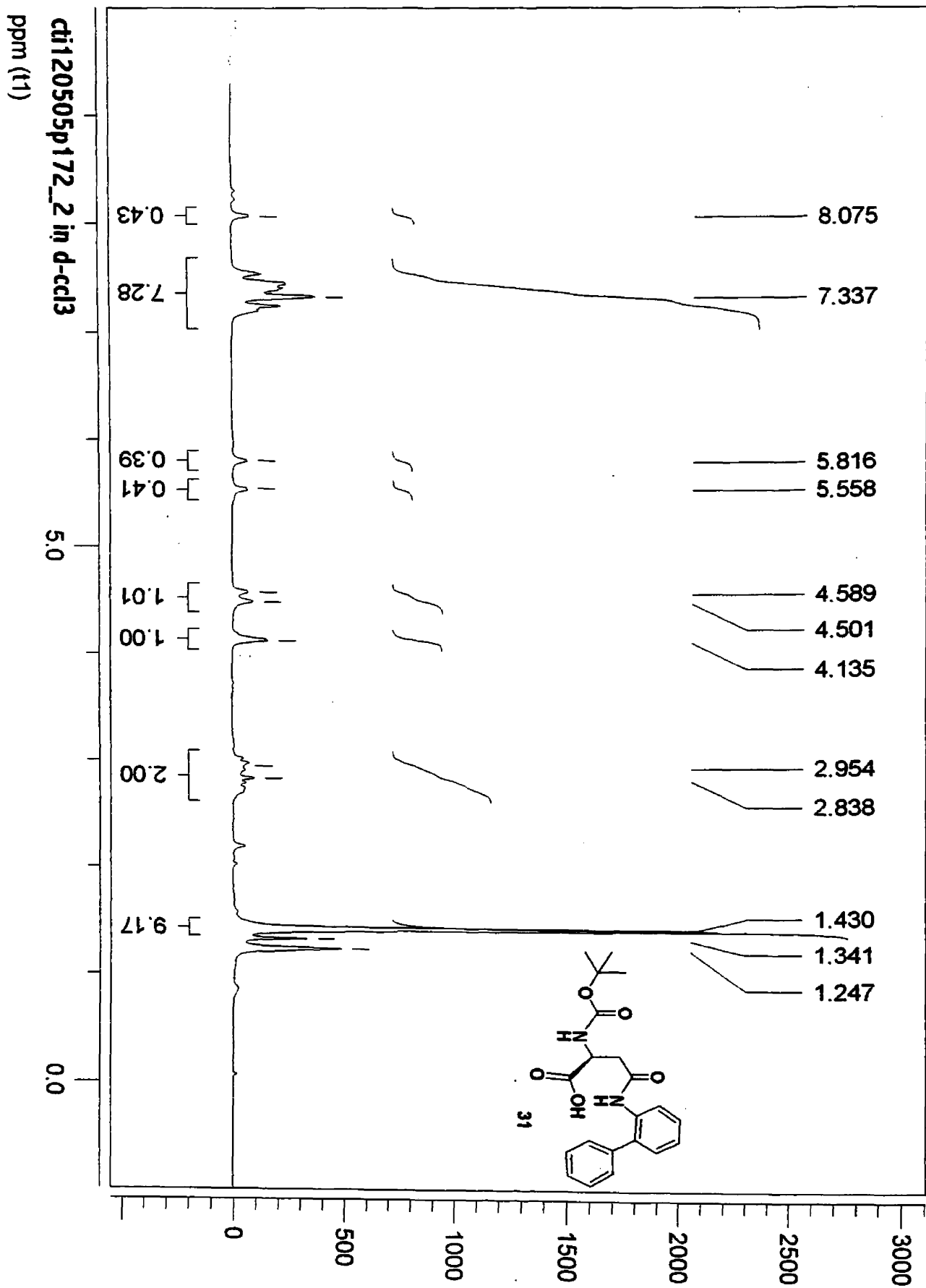


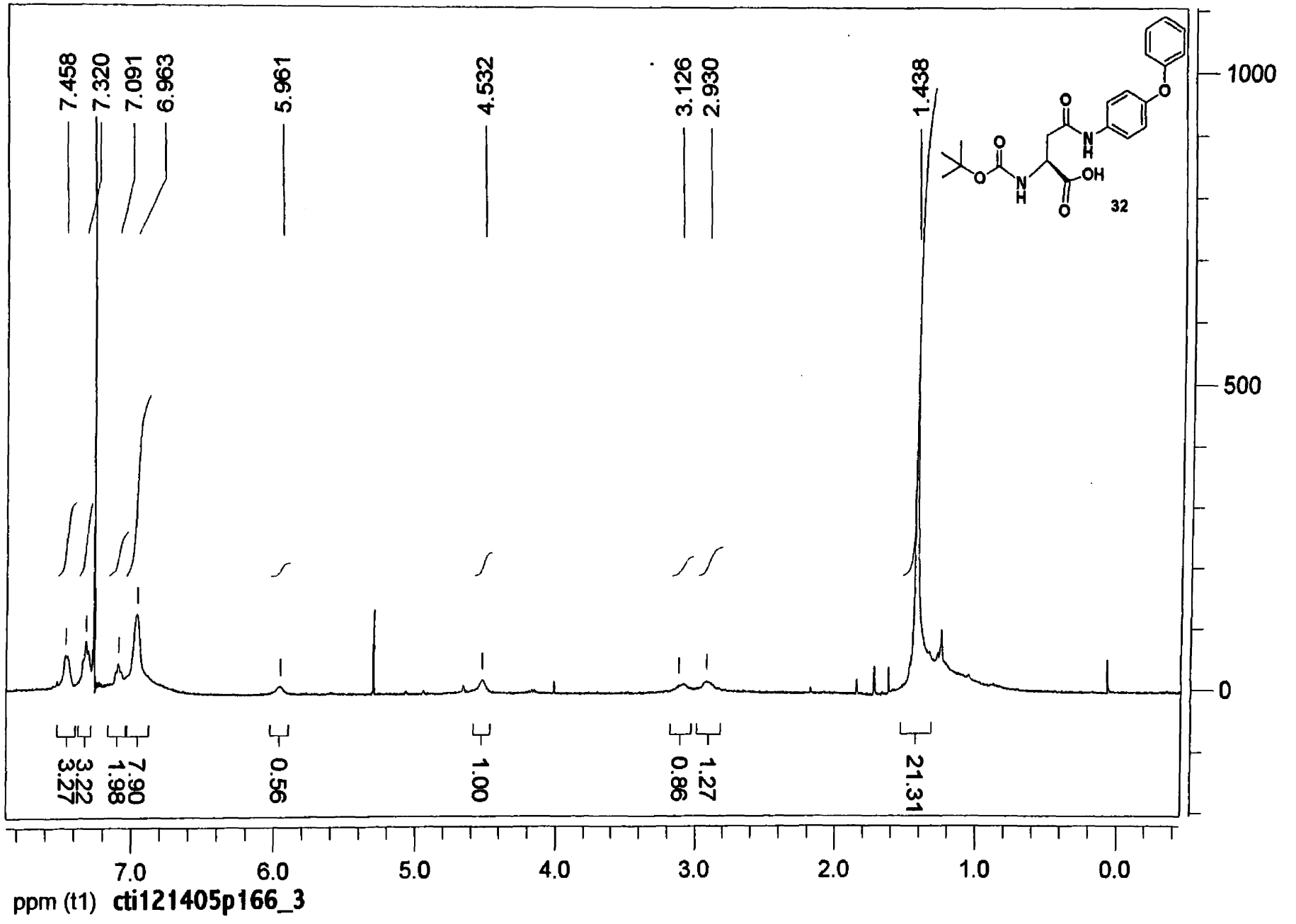
cti101905p136\_1  
ppm (t1)



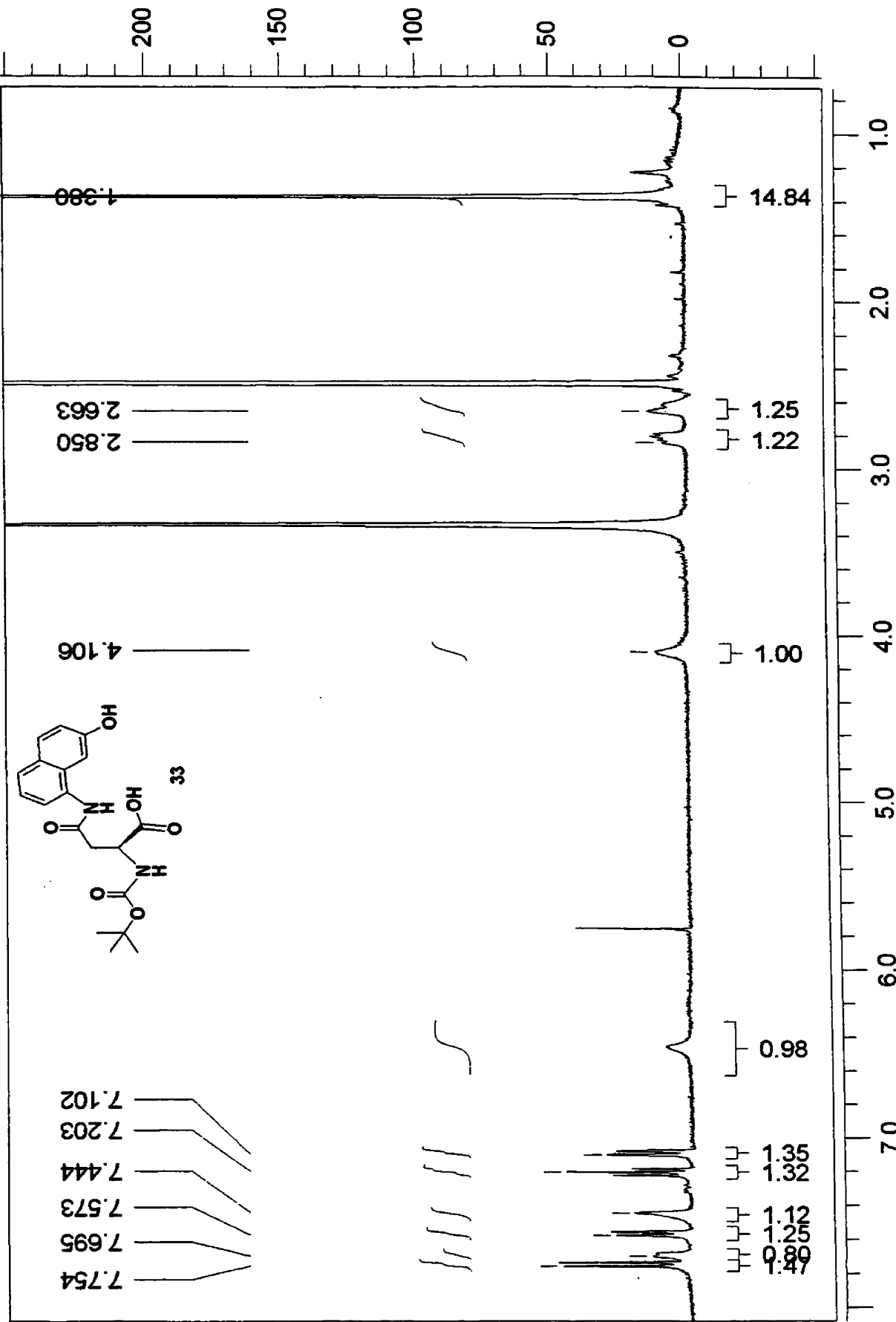




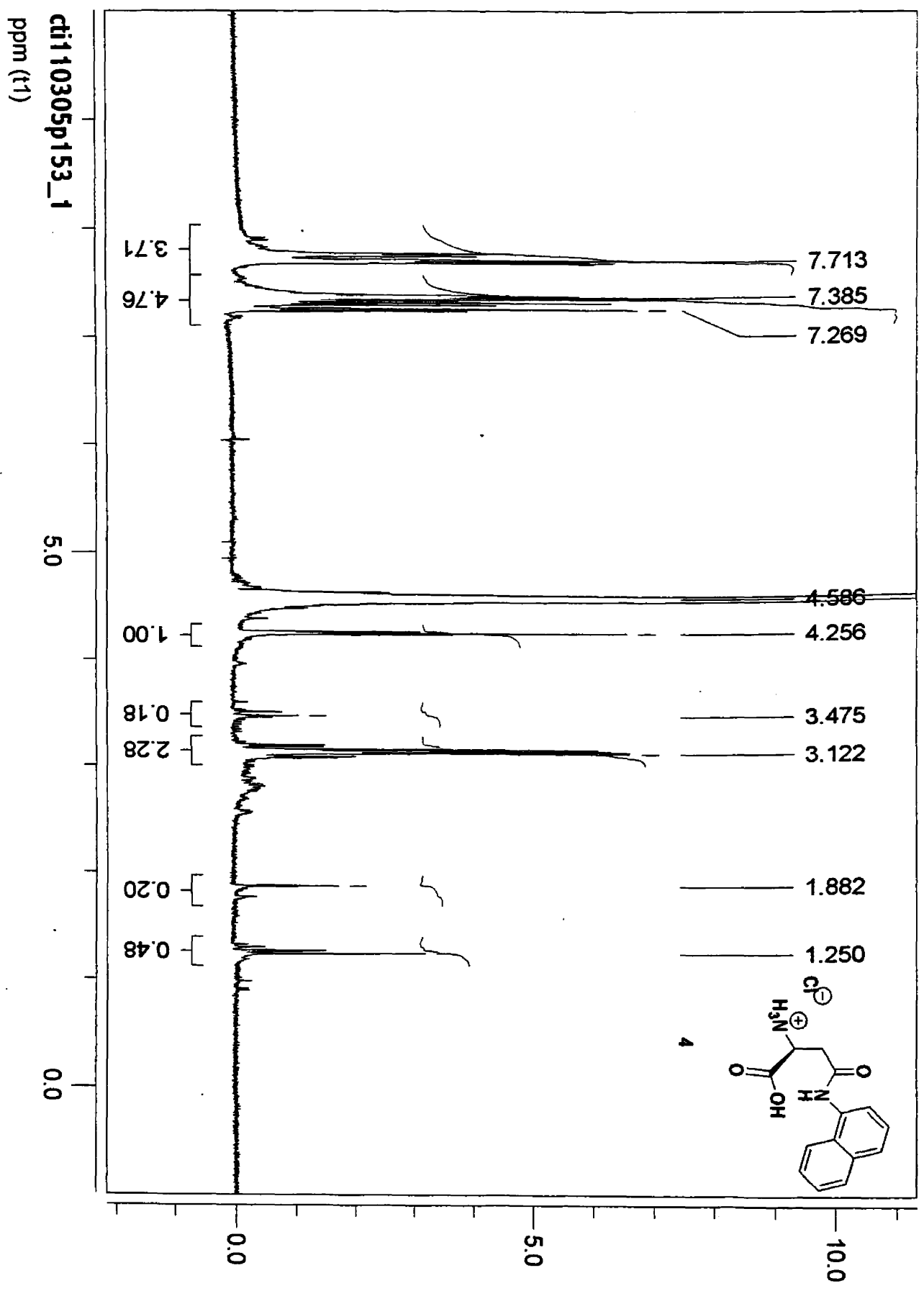








ppm ( $\tau$ ) cti121405p162\_1 in DMSO



ppm (t1) **cti11705p32\_1 in DMSO**

